Building and Environment 239 (2023) 110431

Contents lists available at ScienceDirect

Building and Environment

journal homepage: www.elsevier.com/locate/buildenv

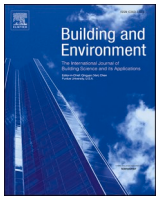

Evaluation on the performance of tree view factor in a high-density subtropical city: A case study in Hong Kong

Ka Yuen Cheng [a,*], Kevin Lau [b], Ying Ting Shek [c], Zhixin Liu [a], Edward Ng [a,c,d]

[a] School of Architecture, The Chinese University of Hong Kong, New Territories, Hong Kong, China
[b] Department of Civil, Environmental and Natural Resources Engineering, Luleå University of Technology, Sweden
[c] Institute of Future Cities, The Chinese University of Hong Kong, New Territories, Hong Kong, China
[d] Institute of Environment, Energy and Sustainability, The Chinese University of Hong Kong, New Territories, Hong Kong, China

ARTICLE INFO

Keywords:
Outdoor thermal comfort
Tree view factor
ENVI-met
Subtropical summer
High-rise metropolis

ABSTRACT

Outdoor thermal comfort is a primary concern when designing urban environments suitable for pedestrian activities. In previous research, urban greenery had been considered as an effective strategy to mitigate the deterioration of the street-level thermal environment. Tree view factor (TVF), a parameter that can estimate the amount of tree cover visible in the overlying hemisphere, was applied in recent thermal environment assessment studies. However, a detailed understanding of TVF's suitability and application in a subtropical high-rise compact metropolis with diversified land uses is still lacking. To fill the knowledge gap, this study used Hong Kong as a study case and conducted ENVI-met simulations to analyse the human thermal comfort at two levels of TVF sites and two weather conditions. Results showed that high TVF (Htvf) sites had a pronounced reduction in mean radiant temperature (TMRT) of at least 15 °C after 12:00 under both typical and extreme weather scenarios. A lower mean physiological equivalent temperature (PET) of below 30 °C and 35 °C remained in the daytime of typical and extreme weather scenarios, respectively. It was also found that low TVF sites inside parks received more solar radiation, while Htvf sites inside parks exhibited a more substantial cooling potential than that inside street canyons. Htvf sites could maintain better pedestrian thermal comfort due to the shading effect. This study also proved that TVF is more suitable than green coverage ratio (GCR) in urban thermal environment assessments and urban green infrastructure design to create a thermally comfortable high-rise and high-density metropolis.

1. Introduction

1.1. Urban greenery and human thermal comfort

Due to the considerable alteration to the original land covers, rapid urbanization is a major factor causing environmental degradation in recent decades. Featuring densely built environments, anthropogenic heat sources and limited green and blue infrastructures, urban areas are expected to experience amplified air temperature warming with very high confidence in projected climates [1]. Intergovernmental Panel on Climate Change (IPCC) Sixth Assessment Report [1] also highlighted the more frequent occurrence of intensified heatwave. According to the Hong Kong Observatory, the annual maximum air temperature of 36.1 °C in 2021 was the third-highest on 138 years' record. It was 0.5 °C lower than the highest record in 2017 [2]. In 2022, the extensive heatwave in Europe was unprecedentedly strong. Air temperature exceeding 40 °C was recorded in the United Kingdom while 47 °C was observed in Portugal [3]. In addition to future climate change, the thermal environment inside urban areas will deteriorate further. Human thermal health and comfort are greatly threatened by heatwaves and extremely hot weather, which may cause discomfort and even heat-related illnesses, including heat syncope, heat exhaustion, and heat stroke [4]. Notably, the human thermal comfort at the pedestrian level (about 1.5 m–2 m height above the ground [5]) should be paid more attention to, as people spend 10% of their summertime outdoors [6], the thermal conditions at that height could influence people's thermal sensation directly. The deterioration of thermal environments in high-density cities [7–9] remains to be serious.

* Corresponding author. Room 505, Lee Shau Kee Architecture Building, The Chinese University of Hong Kong, Shatin, Hong Kong, China.
E-mail addresses: kayuencheng@cuhk.edu.hk (K.Y. Cheng), kevin.lau@ltu.se (K. Lau), 1155079631@link.cuhk.edu.hk (Y.T. Shek), zhixinliu@cuhk.edu.hk (Z. Liu), edwardng@cuhk.edu.hk (E. Ng).

https://doi.org/10.1016/j.buildenv.2023.110431
Received 30 December 2022; Received in revised form 15 May 2023; Accepted 17 May 2023
Available online 18 May 2023

Therefore, many mitigation measures have been developed to cool the city and prevent the worsening of urban pedestrian-level thermal comfort due to extreme heatwave. Urban green infrastructures (UGI) have been identified as one of the most significant nature-based solutions to mitigate and adapt the climate change and the urban heat island effect. They can partly re-establish the ecosystem of evapotranspirative cooling and shading, improve the outdoor thermal comfort, as well as dampen the energy demand for cooling in summer [10]. The thermal benefits of urban trees, grass, shrubs, vertical greening and rooftop greening had been found in numerous studies [11–14]. In a research conducted in Toronto, Canada, it was reported that the air temperature was reduced by 0.8 °C in the high-rise areas on a summer afternoon when the local urban vegetation coverage was increased by 10% by including more trees and grass [15]. Another study in Rome, Italy, by Battista et al. [16] suggested a 0.37 °C decrease in air temperature could be obtained when introducing 34 trees of 10 m in height in the studied square, compared to the base case.

Increasing urban vegetation proportion was reported as a highly effective approach because of its cooling by shading and evapotranspiration [7,17–19]. Tall vegetation can shade the ground level, reducing the air temperature [11,20]. Meanwhile, evapotranspiration can increase the latent heat flux in proximity, regulating the sensible heat flux and the rise in air temperature [11,21,22]. However, it was reported that the presence of trees could reduce wind speed in urban environments [23]. To summarise, urban greenery is influential to the microclimate and the outdoor thermal comfort at the pedestrian level.

1.2. Greenery morphological parameters

To estimate the potential cooling and microclimate effects of vegetation, numerous urban morphological parameters of greenery were examined previously. The green coverage ratio (GCR) is widely scrutinised. It estimates the amount of vegetation cover within a selected buffer area. Previous research showed that GCR and the cooling effect positively correlated. Yang et al. [24] reported that air temperature decreased by 0.2 °C when GCR had a 10% increase in a residential area in Nanjing, China, and the most prominent decrease of 0.3 °C appeared when GCR changed from 30% to 40%. A previous study by Zaki et al. in Kuala Lumpur also highlighted the critical importance of green coverage on cooling [25].

However, GCR accounts effects of both tall trees and short greenery surfaces. It correlates with surrounding thermal conditions to some extent but may not with human thermal comfort at the pedestrian level. In hot and humid subtropical regions, such as Hong Kong, shade provision was crucial to mitigate street-level thermal comfort for pedestrians [7,26–32]. But shrubs and grass were more likely to contribute to cooling at the surface level [25,33]. As suggested by Li et al. [34], the fundamental element affecting air temperature was the tree cover rather than shrub-grass surfaces. Hence it is essential to examine the cooling abilities contributed by trees.

To estimate the effects of tree shading on thermal comfort, various morphological parameters had been examined in previous research. Zhang et al. [35] utilised satellite images to calculate the ratio of tree canopy area to the park surface area and discovered that increased park tree coverage could lead to a dropping park air temperature of 2.5 °C. Nevertheless, this method only provides a rough estimation of tree coverage. Solar radiation can penetrate gaps between leaves and reach the ground surface, affecting thermal comfort at the pedestrian level. Leaf Area Index (LAI) is another popular parameter that measures the total one-sided area of leaf surfaces per unit of ground area. In general, higher LAI could lead to more robust cooling of air temperature [34], attenuation of direct solar radiation [36,37] as well as regulation the thermal comfort [38]. However, research conducted in Busan (Cwa in Köppen-Geiger climate classification), South Korea, concluded that LAI was the least important factor in improving street-level pedestrian thermal comfort among the other six factors regarding canyon geometry (e.g., street orientation) and tree configurations (e.g., tree heights) [39]. As LAI only considers the effect of leaf area on thermal comfort, it neglects the shadow by wide tree trunks, especially when the sun is at a lower altitude.

In some research, hemispheric photos were analysed to quantify the canopy density, particularly of individual trees [40]. This approach considers all the visible tree components in the overlying hemisphere, estimated by the tree view factor (TVF). Its value ranges from 0 (no tree components are visible) to 1 (the sky is completely blocked while no gaps between leaves are observed). Similar concepts of assessing the horizontal tree view factor had been applied in previous psychological research, revealing trees were importantly related to the positive emotions of pedestrians [41]. In the context of microclimate effects, Xue et al. [42] concluded that TVF was significantly associated with the air temperature divergence between the real-time measurement and the official daily mean on a typical summer day. Other weather elements, including relative humidity [43,44], mean radiant temperature [43,45], and land surface temperature [46], had been subjects of previous TVF studies in various climate regions. Besides, the relationship between TVF and outdoor thermal comfort was investigated recently. In Sapporo, Japan, it was revealed that TVF and wet-bulb globe temperature had a negative correlation [47]. The relationship between TVF and other thermal comfort indices such as COMFA [44] and thermal comfort vote (TCV) [48,49] was also been recently discussed. Roadside trees away from building shadings were also investigated using TVF to analyse their effects on the surrounding environment in a tropical city [50].

However, whether TVF is suitable to be used in subtropical high-density cities' urban design is still unclear. Due to their hot-humid climates and complex urban morphologies (high-density, high-rise, and compact urban environments with diversified land uses), it is challenging to create thermal-comfortable urban environments. Previous TVF research often investigated the impacts caused by the tree geometry and morphology without considering the interaction of neighbouring buildings [50] and urban structures. Moreover, previous TVF research usually was conducted under current typical weather and concluded whether TVF was an influential morphological parameter. The suitability of using TVF to evaluate the relationship with different weather elements under extreme weather can be further investigated.

1.3. Objective

This research aims to determine whether the Tree view factor (TVF) is a suitable vegetation morphology parameter for pedestrian thermal comfort assessment in subtropical high-density cities. TVF's performance in Hong Kong, a compact city with a hot and humid climate, was investigated as a case study. This study analysed the performance of TVF under typical and extreme summer weather scenarios, considering the high incidence of heatwaves under global climate change. Moreover, its performance inside different urban environments (parks and two street canyon orientation) is examined with corresponding pairs of high and low TVF sites. In addition, the significance of implementing TVF in urban design is discussed in detail by comparing it to the widely applied parameter GCR.

2. Methodology

2.1. Study location and environments

Hong Kong (22°08′N - 22°35′N; 113°49′E – 114°31′E) is a coastal city located at the southeastern coast of China. In 2021, the population in this highly urbanised city is 7.4 million. Kowloon has the highest population density of 47560 persons per km^2 [51]. Urban morphology is complex. High-density and high-rise buildings of 60 m in height [52] are typical urban structures. Nevertheless, pocket parks and rivers can sometimes be found. With green and blue infrastructures, mixed land uses are concentrated in a small area. In other words, commercial lands

can be next to residential and recreational land use in a small district.

Six locations (Fig. 1) were selected as the study areas. Kowloon City (KLC) and Mong Kok (MK) represent Hong Kong's typical high-density downtown areas with high-rise buildings in the Kowloon Peninsula. Nam Shan Estate and the surrounding neighbourhood (NSE) locates in the Kowloon Peninsula and near the downtown areas. Tuen Mun (TM), Tai Po (TP) and Tin Shui Wai (TSW) are new towns in New Territories, where more trees and water bodies exist. Detailed descriptions of the study locations are listed in Table 1.

2.2. General summer weather in Hong Kong

Hong Kong has a hot and humid subtropical summer (Cfa in the Köppen-Geiger scheme [53]). Starting from May, daily mean air temperature often exceeds 26 °C, with afternoon temperature reaching approximately 30 °C or above, while the monthly mean relative humidity remains 70% or above in the afternoon [54,55].

Background winds are usually moderate. Monthly mean wind speed ranges from 19.8 km/h to 21.6 km/h, measuring at an outlying island named Waglan Island. However, due to obstruction by urban structures, the monthly mean wind speed is weakened to approximately 10 km/h inside the city [54]. As typhoons in summer could often bring strong or gale winds to Hong Kong, the wind speed on a typical fine summer day inside the city may even be weaker.

The monthly mean of daily global solar radiation ranges from 14.46 MJ/m^2 to 17.22 MJ/m^2 [54]. Although the monthly mean cloud amount generally exceeds 70% at the Hong Kong Observatory [54], it does not represent that all those clouds are low clouds. Solar radiation can still penetrate thin high clouds to reach and thus heat the surface. Cloud type data is not provided as a part of the Climate Information Service by the Hong Kong Observatory. Therefore, the related data cannot be retrieved.

Heatwave refers to the persistent abnormal high air temperature that often happens in Hong Kong's summertime [56]. For example, in July 2020, the Very Hot Weather Warning was issued for 467 h continuously in Hong Kong [57], with a high daily maximum air temperature ranging from 32.2 °C to 35.3° [58]. Meanwhile, the surface wind speed is usually low or sometimes stagnant during the heatwave. As a result, the thermal comfort within the city could considerably deteriorate.

Because of different combinations of dense high-rise buildings, compact mixed land covers, and orography in the territories, regional weather may vary in different study areas [59]. Therefore, ENVI-met simulations are used to obtain detailed spatial distributions of various weather elements and the human thermal comfort indicator in the six target locations.

2.3. Microclimate simulation using ENVI-met 5.0

2.3.1. ENVI-met description

ENVI-met, developed by Michael Bruse in 1998 [60], is a holistic three-dimensional microclimate computational fluid dynamics model. As a non-hydrostatic model, ENVI-met can simulate surface-plant-air interaction in an urban environment based on fluid mechanics, thermodynamics, and atmospheric physics principles. Owing to its simplified approach and ability to perform holistic simulation on meteorological variables' diurnal cycle at a lower computational cost, ENVI-met has been utilised worldwide in the recent two decades [61].

Our research team has previously conducted much research in high-rise and high-density cities with a hot and humid climate, in which ENVI-met had been validated and proved to be a suitable simulation model for urban microclimate [37,59,62–65]. An ENVI-met validation paper from our research team concluded that ENVI-met could simulate the air temperature and the mean radiant temperature with a satisfying accuracy during summer daytime. ENVI-met simulations could also replicate the thermal-radiative characteristics of the green infrastructures such as ground trees, green façade and green roofs [66].

2.3.2. Model configuration

In this research, ENVI-met 5.0 Science Version was selected as the simulation tool. Table 2 lists the model details of the six study locations. The resolution was 9 m (horizontal) and 4 m (vertical). Telescoping was applied in vertical grid generation with a 20% telescoping factor and started telescoping after 50 m.

All landscape elements were selected from the default database. Buildings were constructed with concrete (0100C2). Dense trees with

Fig. 1. A Hong Kong map showing the six study locations that are indicated by red squares. The satellite photo shows that the study locations are highly urbanised area. The base map is constructed by using the ArcGIS software. (For interpretation of the references to colour in this figure legend, the reader is referred to the Web version of this article.)

Table 1
General descriptions on building morphology, pedestrian activity, greenery and natural water bodies of the six study locations.

Study area	General descriptions
Kowloon City (KLC)	Typical high-density downtown areas in the Kowloon Peninsula. Buildings are mainly five storeys. Commercial activities often concentrate on the ground floor while the upper floors are for residential purposes. The traffic and pedestrian activities are usually busy inside narrow street canyons. Not much roadside vegetation could be found inside the district. A limited number of small pocket parks, the Kowloon Walled City Park and the Kowloon Tsai Park exist within the study area.
Mong Kok (MK)	Typical high-density downtown areas with high-rise buildings in the Kowloon Peninsula. Buildings exceeding ten storeys are common. The ground floor usually consists of shops and the upper floors are for residential or often commercial purposes. The traffic and pedestrian activities are usually busy inside narrow street canyons. Not much roadside vegetation could be found inside the district. A limited number of small pocket parks and the King's Park Rest Garden exist in the region.
Nam Shan Estate and the surrounding neighbourhood (NSE)	Near the downtown areas in the Kowloon Peninsula. Buildings are less compact than in the downtown area and some new towns. Residential buildings of below ten floors dominate the region. Shops mainly locate at shopping malls. Traffic and pedestrian activities on streets are less busy. Greenery areas and roadside trees are much more than in the downtown area. This area is surrounded by 20–30 storeys high-rise buildings in the neighbouring districts.
Tuen Mun (TM)	A new town in the New Territories. A river is found. Trees are more common, and mostly at the roadside, inside parks, or open areas inside housing estates. Compared to the downtown area, parks are more and larger. Hence, pedestrian activities can be frequently found there. Traffic is less busy. Some shops locate at the podium of residential buildings. Meanwhile, shops can be found on the ground floor and in shopping centres a few storeys high. Residential buildings are mostly 20 to 30 storeys. Schools of five storeys are found in the surrounding of housing estates.
Tai Po (TP)	A new town in the New Territories. Rivers are found. Trees are more common, and mostly at the roadside, inside parks, or open areas inside housing estates. More and larger parks exist, compared to the downtown area. Hence, pedestrian activities can be frequently found there if it is thermally comfortable. Traffic is less busy than downtown. Shops often locate at the podium of residential buildings. Ground floor shops and shopping centres of a few storeys also exist. Residential buildings are approximately 20 storeys.
Tin Shui Wai (TSW)	A new town in the New Territories. Natural water features such as rivers and wetlands are found. Trees are more common, and mostly at the roadside, inside parks, or open areas inside housing estates. Compared to the downtown area, parks are more and larger. Pedestrian activities can be frequently found there. Most shops are located inside shopping centres. Frequent pedestrian activities near malls are often observed. Traffic is less busy than in the downtown area. 30-storey residential buildings are more common. Schools of 5 storeys high are found inside the housing estates.

Table 2
The basic information of the model domain of the six study locations.

Location	Mong Kok	Kowloon City	Tai Po	Tin Shui Wai	Nam Shan Estate and the surroundings	Tuen Mun
Abbreviation	MK	KLC	TP	TSW	NSE	TM
Area (m)	1800 × 1800	1710 × 1710	1740 × 1740	2160 × 2160	1530 × 1530	1530 × 1530
Model Size	200 × 200 × 30	190 × 190 × 28	194 × 194 × 26	240 × 240 × 24	170 × 170 × 27	170 × 170 × 28
Rotation (°)	−10	3	0	0	0	−1
Nesting Grids	7	7	7	7	7	7

10 m (0000T1), 15 m (0000SK) as well as 50 cm height grass (000000) were the three types of vegetation used. There were no rooftop greening and green façade applied in the six locations. The distribution of different ground surfaces was resembled according to the actual road and surface conditions by using materials including unsealed soil (sandy loam) (010000), pavement (concrete) (0100PP), granite pavement (single stone) (0100GS), or asphalt road (0100ST). Water features such as rivers and small ponds were represented by deep water (0100WW).

The model domain was generated according to the actual spatial distribution of buildings, water cover, and vegetation by using the ENVI-met Monde Module. However, it was nearly impossible to perform perfect reconstruction at each point because of the limitation of grids. Besides, simulation instability could often be introduced, especially inside a detailed and complex urban environment. Therefore, fine adjustments to buildings and vegetation distribution were applied by using the ENVI-met Space module to avoid instability and ensure successful simulations. Fig. 2 shows an example of the 3D model domain in Mong Kok (MK), one of the densely built-up areas in the Kowloon Peninsula. Other 3D model domains are displayed in Figure S1 and Figure S2.

2.3.3. *Weather data input for simulation*

The full-forcing mode had been applied in the 21-h simulation (from 00:00 to 21:00 the same day). As regional weather varied simultaneously, the input weather data, including air temperature, relative humidity, and wind speed, at each location were retrieved from the nearest operational automatic weather stations (AWS) established by the Hong Kong Observatory. However, as solar radiation data were unavailable at each AWS, direct shortwave radiation, diffuse shortwave radiation, and longwave radiation data from Meteoblue [67] were utilised.

To examine the impact of heatwave events, simulations were performed under the extreme condition (May 18, 2018) [68] and the typical condition (May 8, 2017). Fig. 3 illustrates the weather observed at the nearest AWS, including air temperature, relative humidity, and wind speed for extreme and typical weather of each study area. A few adjustments to the weather data had been made to avoid crashes and instability of the simulations. Fig. 4 summarises three kinds of solar radiation received in Hong Kong. The input solar radiation data are the same for all six study areas.

2.4. *Urban greenery morphological parameters*

Urban morphology parameters had been widely applied in urban-microclimate-related studies [52,69–71] to understand the impact of urban morphology on microclimates. The parameters often help translate scientific findings of climatic phenomena into practical urban designs [69].

Except for upward view factors, a buffer circle with a 100 m radius was used due to two reasons. First, canyon size (30 × 200 m), suggested

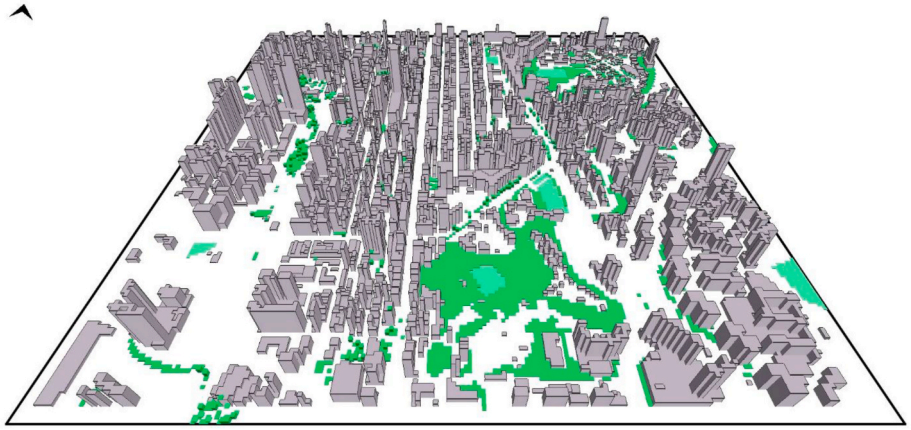

Fig. 2. The 3D model domain of Mong Kok (MK).

by T.R. Oke's urban climate scale classification [72], was a suitable horizon length scale to represent the pedestrians' bio-climate. Second, this buffer size had been applied in numerous research on similar topics [73,74].

2.4.1. Tree view factor (TVF)

TVF quantifies the amount of immediate tree cover obscuring the sky at a given point from a horizontal surface. It varies from 0 to 1, where 0 represents no tree can be observed. Similar to the sky view factor, TVF can be calculated by analysing hemispheric photos. However, as modifications to vegetation had been performed in the model domain, the domain's TVF and the actual ones in the urban environment might differ. Therefore, another approach was used to retrieve TVF from simulations. In ENVI-met, the simulation outcome included the upward vegetation view factor at each grid. As green façades and green roofs were not included in the model designs, the upward vegetation view factor retrieved at 2 m above ground surface could thus be analysed as TVF.

2.4.2. Green coverage ratio (GCR)

GCR refers to the vegetation coverage within the buffer circle at a horizontal surface, and it ranges from 0 to 1. Sometimes percentage representation is used in some research.

In this study, GCR was extracted from the model domains using the counting technique of pixels. Inside the domain, 10 m and 15 m height dense trees and 50 cm height grass were green grids. The GCR at a given point in the model domain was estimated by counting the green pixels within the buffer circle. As there was a lack of detailed spatial vegetation distribution maps in the geographic information product, and the location of vegetation might have been minor adjusted as well, GCR was obtained using the pixels-counting approach. It could approximate the vegetation coverage of the domain more precisely. As green façades and green roofs were not included in the model domains of the six study areas, GCR calculated in this study referred to the ground-level values only.

2.5. Data collation

2.5.1. Site selection for data analysis

Tree grids and exposed grids were identified from the model domain. A tree grid referred to a grid with dense trees of 10 m or 15 m. The latter referred to a grid that was unsealed soil (sandy loam), pavement (concrete), granite pavement (single stone), or asphalt road. In addition, exposed grids did not contain any buildings, vegetation, or water surface.

To obtain more accurate results, grids within 100 m of the model boundary were not considered. Besides, grids within 100 m of the water surface were also neglected in the site selection to achieve a fair comparison.

For data analysis, ten tree grids and ten exposed grids were randomly chosen following the above restrictions in the six locations: KLC, MK, NSE, TM, TP, and TSW. Therefore, there were a total of 120 sites for data analysis. Besides, paired sites within special urban environments such as parks, north-south roads (N–S), and east-west roads (E-W) were also considered. There were six pairs of parks, four pairs of N–S, and five pairs of E-W.

As a result, two groups were classified with the location's TVF. The high TVF (Htvf) group consisted of all 60 sites under a tree, with each TVF larger than 0.6. While for the low TVF (Ltvf) sites, the TVF value of each site was less than 0.3. Fig. 5 shows the 2D model domains with the indication of Ltvf sites, Htvf sites, and the examples of urban environments examined.

2.5.2. Weather data from ENVI-met simulation results

Three weather elements, air temperature (TA), wind speed (WS), and mean radiant temperature (TMRT), were extracted from the hourly simulation results at 2 m above horizontal ground. WS data were extracted to inspect the impact of trees on the ventilation flow. TMRT data were retrieved to scrutinise the cooling effect brought by shading.

2.5.3. Human thermal comfort assessment

Developed based on the Munich Energy-Balance Model for Individuals, physiological equivalent temperature (PET) is defined as the air temperature at which the human skin and core temperature are equal, and the body heat balance is maintained in the assessed environment [75,76]. It describes human thermal comfort by using degrees Celsius.

PET was the indicator for this study for two reasons. Firstly, its calculation considered a variety of meteorological variables (air temperature, relative humidity, wind speed, and mean radiant temperature) and human elements (such as clothing level and metabolic rate caused by activity) [75]. Secondly, PET was a widely used thermal comfort indicator in urban microclimate research in different climatic regions [8,77–79].

PET was calculated by using the BIO-met module in the ENVI-met. The default setting on body parameters and persons metabolism were adopted, i.e., a male aged 35 with 75 kg in weight and 1.75 m in height, and his total metabolic rate is 164.49 W. For the static clothing insulation, 0.4 was used to represent the typical clothing of Hong Kong citizens in the hot and humid summer [65].

Previous research in Hong Kong reported that the neutral PET was 28.1 °C [80] while PET of 32 °C was at which pedestrians would feel slightly warm [81] and still be comfortable [65]. Regarding heat tolerance, ideal thermal stress was defined when PET is lower or equal to

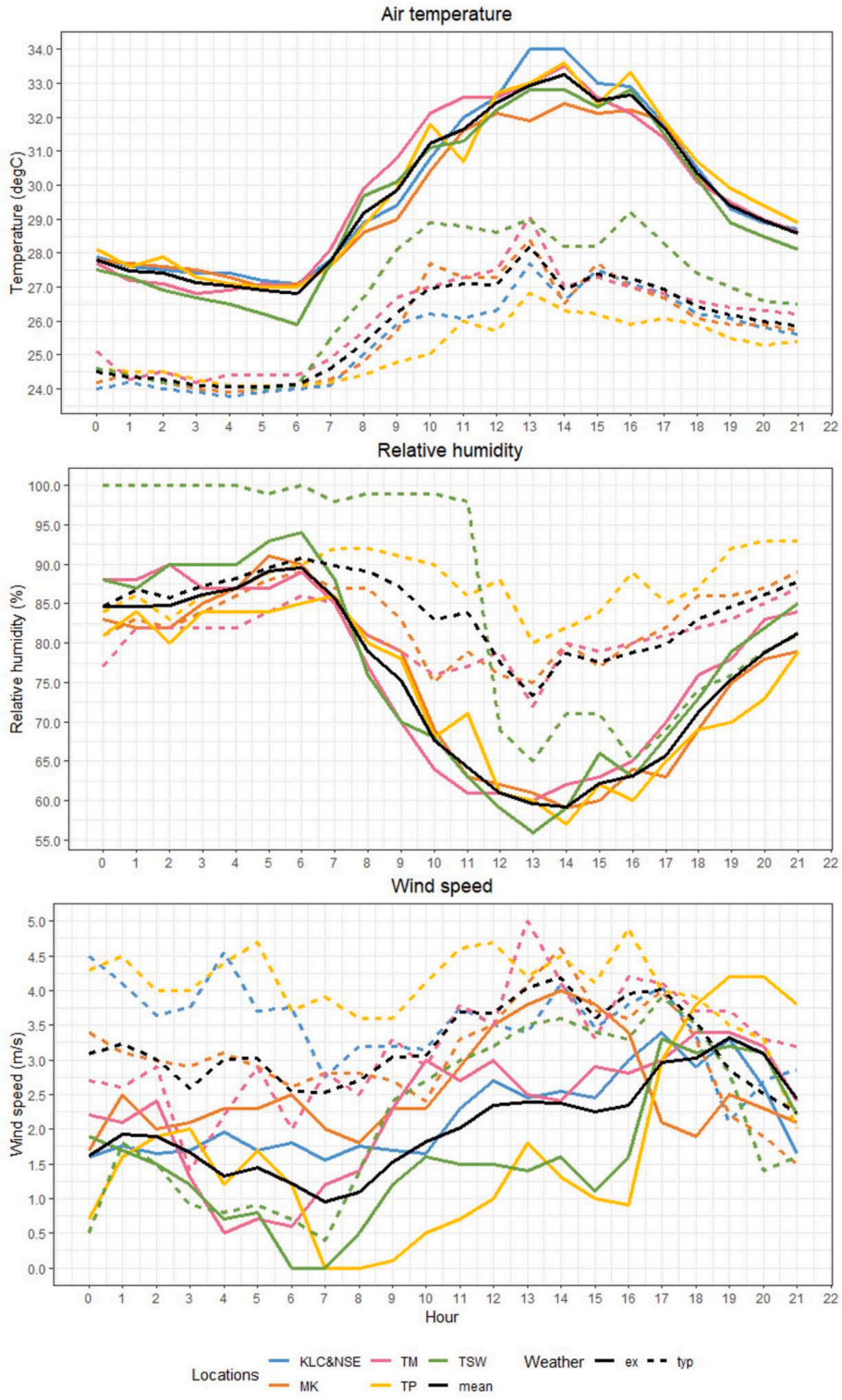

Fig. 3. The weather observed at the nearest AWS of the six study locations. KLC and NSE had the same data due to their similar proximity to the same AWS.

32 °C, while PET higher than 32 °C would be considered a non-ideal condition in this study.

2.6. Scenario descriptions

Data of 09:00, 12:00, and 15:00 represented situations in the morning, noon, and afternoon respectively. Six scenarios had been proposed to study the differences induced by extreme weather conditions at different times of the day, as listed in Table 3.

2.7. Multiple linear regression of PET

To evaluate the impact of the urban morphology on the outdoor pedestrian-level thermal comfort, multiple linear regressions were conducted based on the following equation:

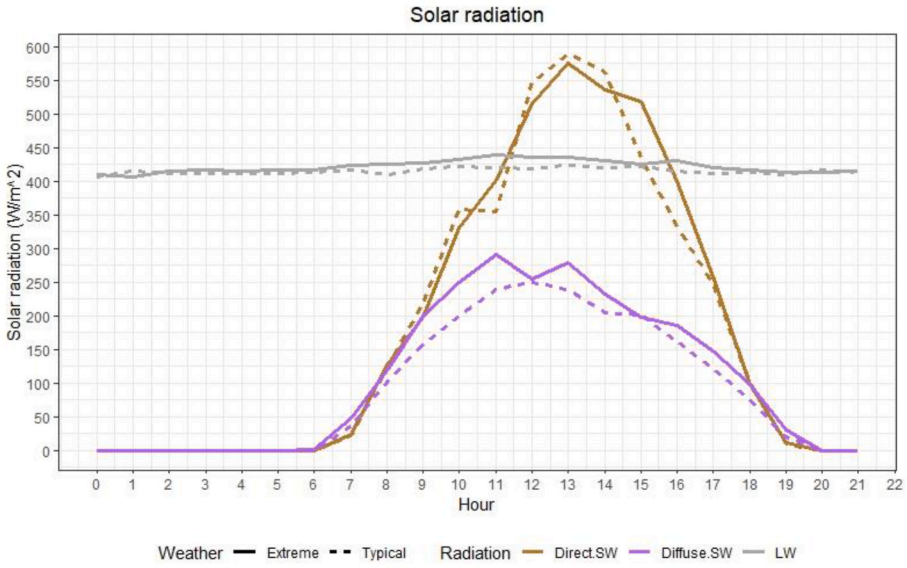

Fig. 4. Input solar radiation data under the two weather scenarios. SW refers to shortwave radiation while LW refers to longwave radiation.

$$PET = aTVF + bBVF_c + c,$$

where *PET* is the value of PET at different time of the day, *TVF* is the tree view factor (only constituted by vegetation), *BVFc* is the upward building view factor without the presence of any vegetation (only constituted by buildings), *a* and *b* are the corresponding coefficients, and *c* is the intercept.

The mean BVFc of the 60 Htvf sites and 60 Ltvf sites were 0.41 and 0.49, respectively. BVFc represented the urban morphology in this study because of the following considerations: 1) The significant correlation between BVFc and intra-urban climates in high-rise and high-density cities had been proved [82], thereby allowing BVFc to be a viable indicator to investigate the relationship between urban morphology, urban microclimate, and human thermal comfort. 2) Among common urban morphology parameters in microclimate research, BVFc was relatively straightforward to be obtained and accurately calculated for a specific location using ENVI-met. A previous study [83] has summarised twelve frequently applied parameters, including building coverage ratio, building volume density, mean building height, floor area ratio, and frontal area index. However, most of these parameters could not be easily and accurately extracted from ENVI-met models.

The multiple linear regressions were conducted with data extracted from the six case scenarios mentioned in section 2.6. Two series of regressions were performed. One was performed with 120 sites, while another analysed the 30 sites in the special urban environments (i.e., E-W, N–S and park). The model was significant at 0.05 level.

3. Results

3.1. Scenario analysis

Tables 4 and 5 summarise the meteorological variables at all 120 Ltvf and Htvf sites. Fig. 6 illustrates the boxplot distribution of the microclimate variables in different sites under the six scenarios.

3.1.1. Typical weather condition

The following section highlighted characteristics of Ltvf and Htvf sites in typical weather scenarios (09typ, 12typ, and 15typ).

Similar air temperatures were observed at Ltvf and Htvf sites in the three scenarios. The difference between the mean of Ltvf and Htvf sites slightly varied from nearly 0.1 °C (in the morning) to 0.2 °C (at noon and in the afternoon).

In all three scenarios, light winds of less than 3 m/s were observed in all sites. Moreover, Ltvf sites generally had higher wind speeds, implying that the presence of trees would slow the ventilation flow.

Htvf sites had prominently reduced TMRT. The mean TMRT of Htvf sites remained under 33 °C in all three scenarios. Regarding the difference between the mean of Ltvf and Htvf sites, it enlarged from 7.4 °C in the morning to 16.2 °C at noon. Therefore, it implied that TMRT reduction could be strengthened during the period with the strongest insolation and maintained throughout the daytime due to the high effectiveness of tree shading.

PET at Htvf sites was prominently lower. While the mean PET at Ltvf site reached 36.4 °C during the daytime, the mean PET could remain under 32 °C at Htvf sites. It indicated the non-ideal thermal sensation (above the 32 °C, the slightly warm threshold) for pedestrians to stay at Ltvf sites during daytime. Whereas staying at Htvf sites could allow an ideal thermal sensation throughout the day. Moreover, the advantage of staying at Htvf sites became more prominent in the hottest period of the day. In the morning, the difference between the mean of Ltvf and Htvf sites was 1.9 °C. This difference enlarged to 7.1 °C and 6.6 °C at noon and afternoon, respectively.

3.1.2. Extreme weather condition

The following section reported characteristics of Ltvf and Htvf sites in extreme weather scenarios (09ex, 12ex, and 15ex).

Similar air temperatures were observed at Ltvf and Htvf sites in the three scenarios. The difference between the mean of Ltvf and Htvf sites increased from 0.1 °C in the morning to 0.31 °C in the afternoon.

Wind speeds at all sites were less than 3 m/s during the heatwave, with lower WS at Htvf sites. The difference between the mean of the two groups of sites varied from 0.1 m/s to 0.2 m/s.

TMRT had a marked reduction at Htvf sites due to the existence of trees. The mean TMRT at Htvf sites ranged from 27.6 °C in the morning to 35.4 °C at noon. Meanwhile, the mean TMRT varied from 36.5 °C in the morning to 52.4 °C at noon at Ltvf sites. The difference between the mean of Htvf and Ltvf sites was 8.9 °C in the morning, 17.0 °C at noon, and 15.0 °C in the afternoon. It suggested that TMRT reduction by trees was still effective during heatwaves.

The substantial PET reductions at Htvf sites were notable. The daytime mean PET at Htvf sites ranged from 28.3 °C to 34.6 °C, while those at Ltvf sites varied from 32.4 °C to 44.9 °C. The difference between the mean of sites increased from 4.1 °C in the morning to 10.3 °C at noon and 9.3 °C in the afternoon. The hottest Ltvf and Htvf sites had a

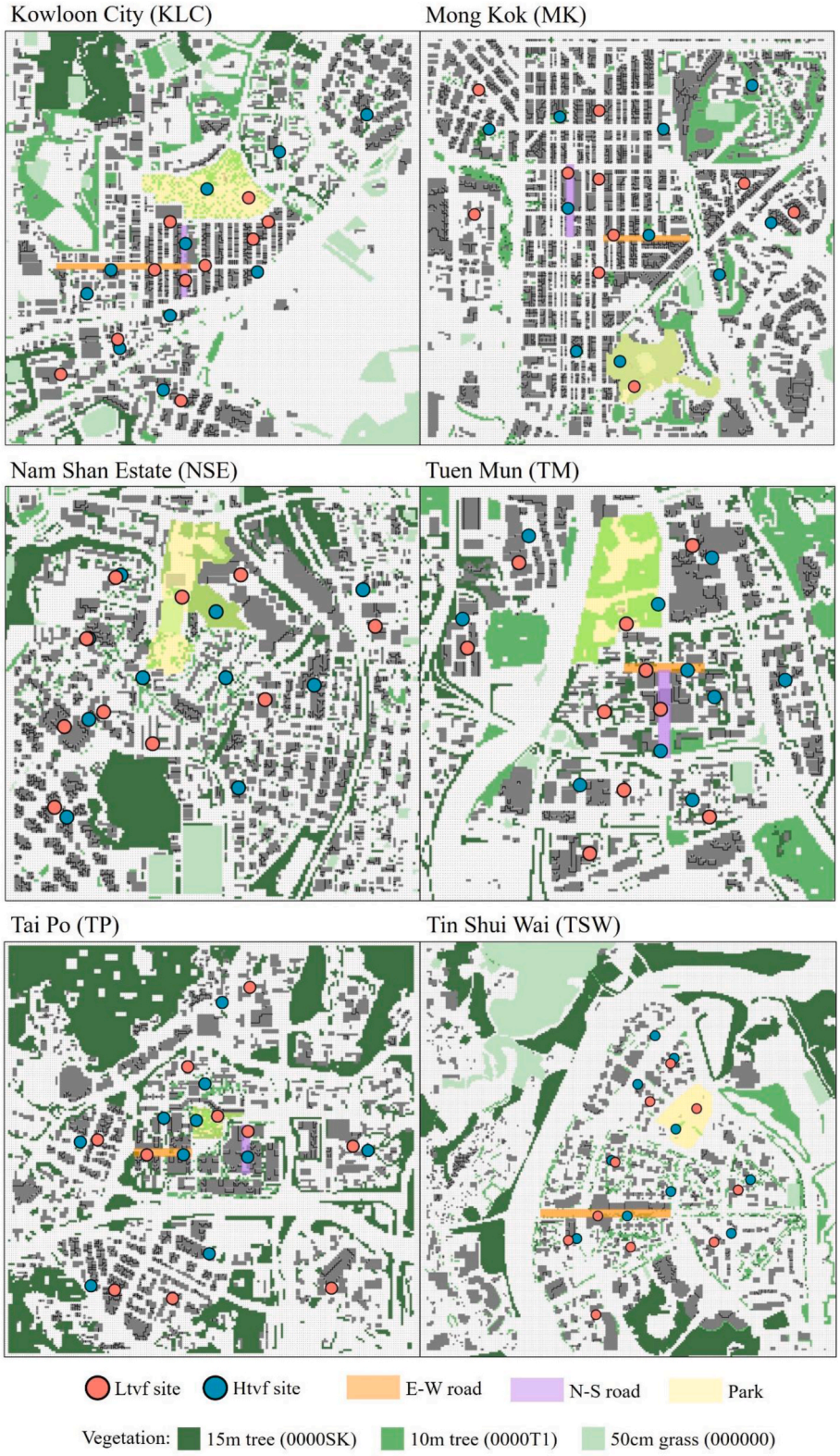

Fig. 5. The 2D domains of the six locations. The orange, purple, and yellow shades illustrate examples of E-W road, N–S road and park, respectively. The pink and blue points overlaying on the shades are the corresponding pair of Ltvf and Htvf sites inside the three special urban environments. (For interpretation of the references to colour in this figure legend, the reader is referred to the Web version of this article.)

considerable difference of 17 °C in the afternoon. It implied that Htvf sites were better thermal environments during heatwaves compared to Ltvf sites. Nevertheless, although the daytime PET reductions were remarkable at Htvf sites, only morning was the thermally ideal period for outdoor activities.

3.1.3. *Heatwave event impacts*

By comparing the characteristics concluded in section 3.1.1 and

Table 3
The six case scenarios and its naming.

	Typical weather condition	Extreme weather condition (heatwave)
Morning	09typ	09ex
Noon	12typ	12ex
Afternoon	15typ	15ex

3.1.2, the impact caused by heatwave events were reported in this section.

During heatwaves, daytime TA in both Htvf and Ltvf sites was prominently higher than usual. In the morning, the mean increase in TA was 3.3 °C for both sites. It was noteworthy that the mean increase at noon and in the afternoon was approximately 5 °C (intensified by nearly 2 °C compared to the morning values). The maximum increase due to heatwave impact at Htvf and Ltvf sites was both 4.8 °C in the morning while they were 7.3 °C and 7.2 °C at noon, respectively. It suggested that ground-level heating could intensify during heatwave events. Besides, heatwaves could cause a slightly larger difference between the mean TA of Htvf and Ltvf sites (particularly at noon and in the afternoon), implying a more heterogeneous air temperature distribution due to the impact of heatwaves.

WS at Ltvf sites notably weakened during heatwaves. Mean reductions of 0.3 m/s to 0.5 m/s were found in Ltvf sites during the daytime, while no clear reduction trend was observed at Htvf sites. As illustrated in Fig. 6b, Ltvf and Htvf sites had a more similar WS during heatwaves. Hence no prominent difference between the mean of these two groups could be observed.

TMRT did not prominently changed during heatwaves. For Ltvf sites,

Table 4
Summary of air temperature (TA) and wind speed (WS). Overall refers to the overall statistics of total 120 sites regardless of the classification of sites. Max refers to the maximum value while min refers to the minimum value. Sd refers to the standard deviation.

	TA	Ltvf	Htvf	Overall		WS	Ltvf	Htvf	Overall
09typ	max	28.4	28.2	28.4	**09typ**	max	2.3	1.9	2.3
	min	25.1	25.1	25.1		min	0.1	0.0	0.0
	mean	26.4	26.4	26.4		mean	1.0	0.5	0.8
	sd	0.91	0.88	0.90		sd	0.56	0.45	0.56
09ex	max	30.8	30.8	30.8	**09ex**	max	1.8	1.8	1.8
	min	29.0	28.7	28.7		min	0.1	0.1	0.1
	mean	29.8	29.6	29.7		mean	0.6	0.4	0.5
	sd	0.45	0.43	0.44		sd	0.39	0.31	0.36
12typ	max	31.5	31.1	31.5	**12typ**	max	2.5	1.8	2.5
	min	26.8	26.6	26.6		min	0.0	0.0	0.0
	mean	28.9	28.7	28.8		mean	1.1	0.6	0.9
	sd	1.15	1.13	1.14		sd	0.61	0.46	0.59
12ex	max	35.3	34.9	35.3	**12ex**	max	2.4	2.6	2.6
	min	33.3	32.4	32.4		min	0.1	0.0	0.0
	mean	34.2	33.8	34.0		mean	0.8	0.7	0.8
	sd	0.47	0.47	0.50		sd	0.59	0.50	0.55
15typ	max	31.4	31.1	31.4	**15typ**	max	2.6	1.8	2.6
	min	27.2	26.9	26.9		min	0.0	0.0	0.0
	mean	29.5	29.3	29.4		mean	1.0	0.6	0.8
	sd	0.98	0.94	0.97		sd	0.59	0.43	0.57
15ex	max	36.2	35.7	36.2	**15ex**	max	2.3	2.3	2.3
	min	33.2	33.1	33.1		min	0.0	0.0	0.0
	mean	34.6	34.3	34.4		mean	0.7	0.6	0.6
	sd	0.72	0.67	0.71		sd	0.56	0.44	0.50

Table 5
Summary of mean radiant temperature (TMRT) and physiological equivalent temperature (PET).

	TMRT	Ltvf	Htvf	Overall		PET	Ltvf	Htvf	Overall
09typ	max	43.5	31.4	43.5	**09typ**	max	34.2	28.2	34.2
	min	24.7	21.0	21.0		min	22.0	22.4	22.0
	mean	32.5	25.1	28.8		mean	26.4	24.5	25.5
	sd	4.54	2.50	5.21		sd	2.52	1.29	2.20
09ex	max	48.4	34.3	48.4	**09ex**	max	38.3	32.2	38.3
	min	28.8	22.8	22.8		min	28.5	26.3	26.3
	mean	36.5	27.6	32.0		mean	32.4	28.3	30.3
	sd	4.70	2.56	5.85		sd	2.27	1.27	2.77
12typ	max	59.9	41.9	59.9	**12typ**	max	48.7	36.9	48.7
	min	33.1	23.4	23.4		min	29.1	24.1	24.1
	mean	48.5	32.3	40.4		mean	36.4	29.3	32.8
	sd	4.78	6.05	9.77		sd	3.51	3.38	4.96
12ex	max	62.5	42.0	62.5	**12ex**	max	54.9	38.7	54.9
	min	36.8	26.0	26.0		min	36.1	30.0	30.0
	mean	52.4	35.4	43.9		mean	44.9	34.6	39.7
	sd	4.49	4.99	9.75		sd	3.96	2.60	6.14
15typ	max	58.5	38.5	58.5	**15typ**	max	43.5	34.6	43.5
	min	30.1	24.4	24.4		min	27.8	24.3	24.3
	mean	45.6	30.5	38.0		mean	35.6	29.0	32.3
	sd	6.57	4.08	9.32		sd	3.76	2.25	4.51
15ex	max	61.1	42.5	61.1	**15ex**	max	56.2	39.3	56.2
	min	34.0	27.9	27.9		min	34.5	31.1	31.1
	mean	49.4	34.3	41.8		mean	43.8	34.5	39.2
	sd	6.86	3.84	9.36		sd	5.28	2.01	6.12

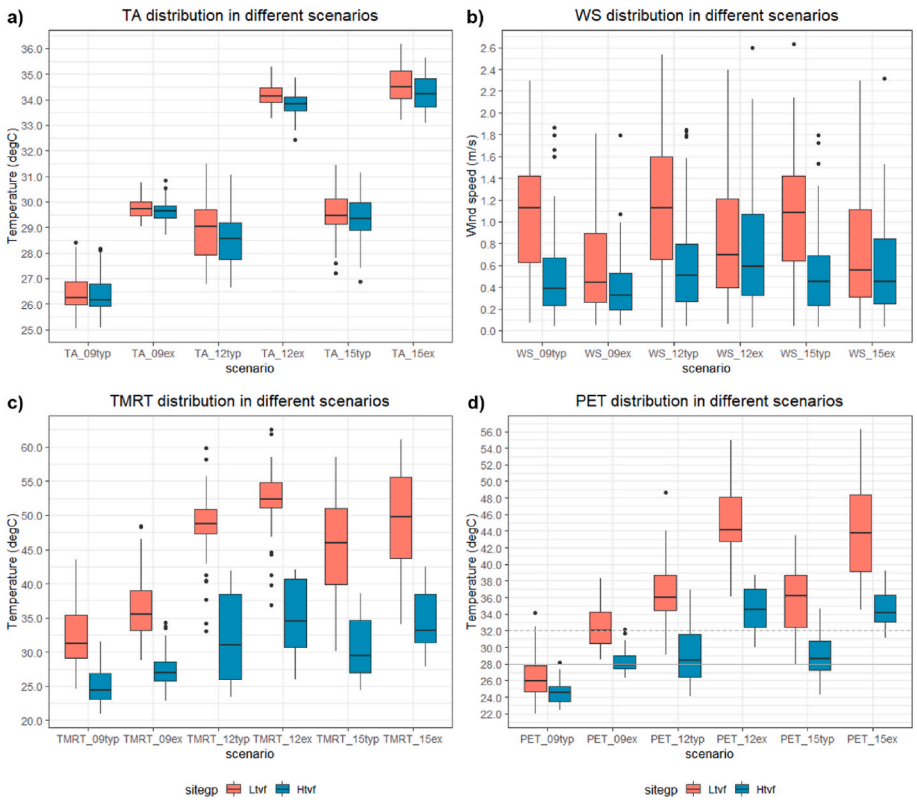

Fig. 6. Boxplot distribution of a) air temperature (TA), b) wind speed (WS), c) mean radiant temperature (TMRT), and d) PET at Ltvf (red) and Htvf sites (blue). For d) PET, the solid horizontal line indicates the neutral PET of 28 °C, while the dotted horizontal line at 32 °C indicates the beginning of non-ideal thermal stress. Sitegp in the legend introduces the two groups of sites. DegC refers to the unit of temperature (°C). (For interpretation of the references to colour in this figure legend, the reader is referred to the Web version of this article.)

it was approximately 4 °C higher than usual. For Htvf, the increase ranged from 2.5 °C to 3.8 °C. In addition, the differences between the mean of Htvf and Ltvf sites slightly changed by +1.5 °C in the morning, +0.8 °C at noon, and no change in the afternoon when compared to the differences under the typical weather. To conclude, during heatwaves, the respective TMRT rises at both sites as well as the differences between the mean of the two groups were slightly higher than usual.

With the above changes in the weather parameters, PET deteriorated at both sites under heatwaves. Compared to the mean PET under typical weather, it was 3.7 °C higher at Htvf sites and 6.0 °C higher at Ltvf sites in the heatwave morning. It was 5.5 °C higher at Htvf sites and 8.2 °C higher at Ltvf sites in the afternoon. Moreover, the differences between the mean of Htvf and Ltvf sites during heatwaves enlarged by 2.3 °C in the morning and 3.1 °C at noon when compared to the usual. The morning cases showed that heatwaves had already influenced thermal comfort, even though the urban environment had not yet received the strongest insolation. Besides, the PET in the heatwave morning was similar to that at noon and afternoon under typical weather conditions (see Fig. 6). Fig. 6 also illustrated that it was not ideal for performing outdoor activities during heatwave noon and afternoon, even if pedestrians stayed under tree shades. Therefore, it implied that the current vegetation distribution might not be sufficiently effective to maintain outdoor thermal comfort in such dense and high-rise urban, especially when heatwaves would become more frequent because of future climate change. Additional mitigations, such as ventilation corridors and water cooling systems, should be introduced to ameliorate the future deterioration of urban thermal environments.

3.2. Diurnal variation analysis

In this section, diurnal variations of weather elements in different urban environments, including urban parks (park), east-west oriented roads (E-W), and north-south oriented streets (N–S), were summarised. The diurnal data of the corresponding pairs of Ltvf and Htvf sites within these three urban environments were extracted and analysed. The cooling maximum was also calculated to show the potential cooling with the presence of overhead trees.

3.2.1. Air temperature

Fig. 7 (top) displays the diurnal variations of air temperatures. For Ltvf sites, similar temperatures were observed in the three environments at noon despite the weather. In the afternoon, parks had slightly higher TA, while TA at N–S was the lowest. It might be due to the degree of building shade from the deep street canyon. Without the shade of buildings, Ltvf sites at parks received more direct solar radiation and surface heating during the daytime. For Htvf sites, the TA of parks was lower than the street by approximately 0.5 °C at noon during heatwave daytime. However, similar temperatures were observed in all sites under typical weather.

Fig. 7 (top) also shows the cooling maximum in air temperature. It indicated that the most substantial cooling occurred in parks (0.6 °C under typical weather and 0.9 °C under extreme weather), followed by E-W and then N–S. All three urban environments showed a larger cooling potential during heatwaves. Although the park's Ltvf sites had higher TA than others, they exhibited a more substantial cooling during the daytime. It was also contributed by the park's Htvf sites, which had relatively lower TA than that inside street canyons with a longer time.

3.2.2. Wind speed

Fig. 7 (bottom) shows the diurnal variation of wind speed (WS) in the three urban environments during heatwaves and typical weather. During most of the daytime, WS was similarly weak. Under typical weather, E-W had the lowest WS at both Htvf and Ltvf sites. When during heatwaves, WS patterns inside street canyons differed. Similar WS was observed between the Ltvf and Htvf sites at E-W. Besides, the Htvf sites at N–S surprisingly showed a slightly higher WS than the Ltvf sites. It demonstrated that the weakened background WS during heatwaves could generate a more similar WS between Ltvf and Htvf sites within deep street canyons. Park was less affected by this impact due to its more open exposure.

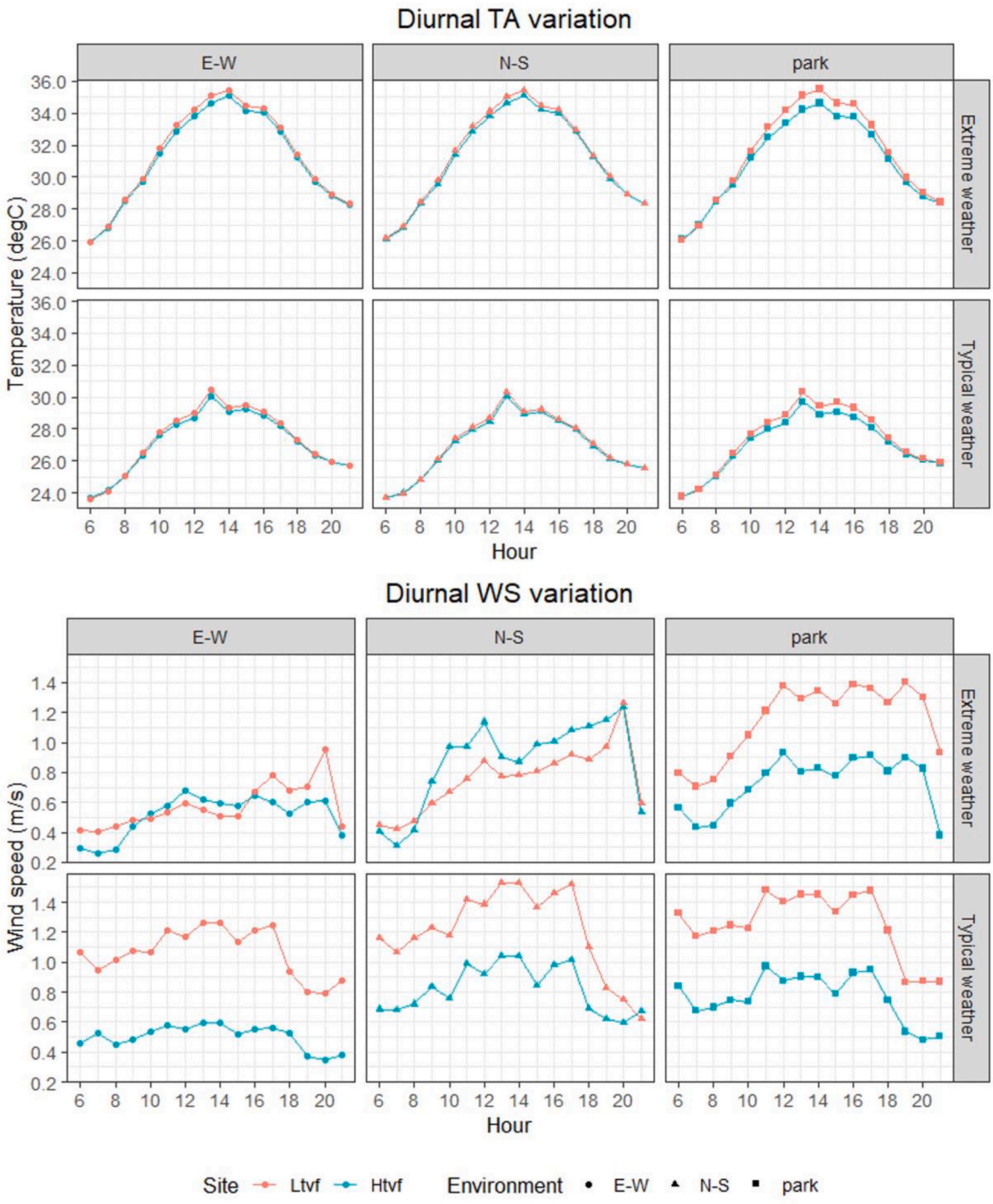

Fig. 7. Diurnal TA (top) and WS (bottom) variation at different urban environments under the two weather conditions. DegC refers to the unit of temperature (°C).

Under typical weather, Ltvf sites at all three urban environments had higher mean wind speeds of approximately 0.5 m/s than Htvf sites. The most considerable wind speed reduction by Htvf sites was found inside parks.

3.2.3. TMRT

Fig. 8 (top) shows the diurnal variation patterns of TMRT. For Ltvf sites under both weather conditions, parks had the highest TMRT, followed by E-W and N–S. The parks chosen were less surrounded by high-rise buildings, resulting insufficient shading to the park's Ltvf sites. Therefore, its TMRT was higher than that located inside deep street canyons. The lowest TMRT of the N–S was likely contributed by the sufficient shading from neighbouring high-rise buildings. It suggested the influencing role of shading from neighbouring high-rise buildings on TMRT. Regarding Htvf sites, similar TMRT were observed in all three urban environments. It might imply that TMRT in different urban environments could be reduced to a similar level with the presence of trees.

Fig. 8 (top) also illustrates the maximum reduction in TMRT under two weather conditions. Parks exhibited the highest maximum reduction (24.0 °C under typical weather and 25.5 °C under extreme weather), followed by E-W (18.6 °C under typical weather and 17.8 °C under extreme weather) and then N–S (10.3 °C under typical weather and 12.1 °C under extreme weather). The difference in TMRT reduction between heatwave and typical weather was not prominent.

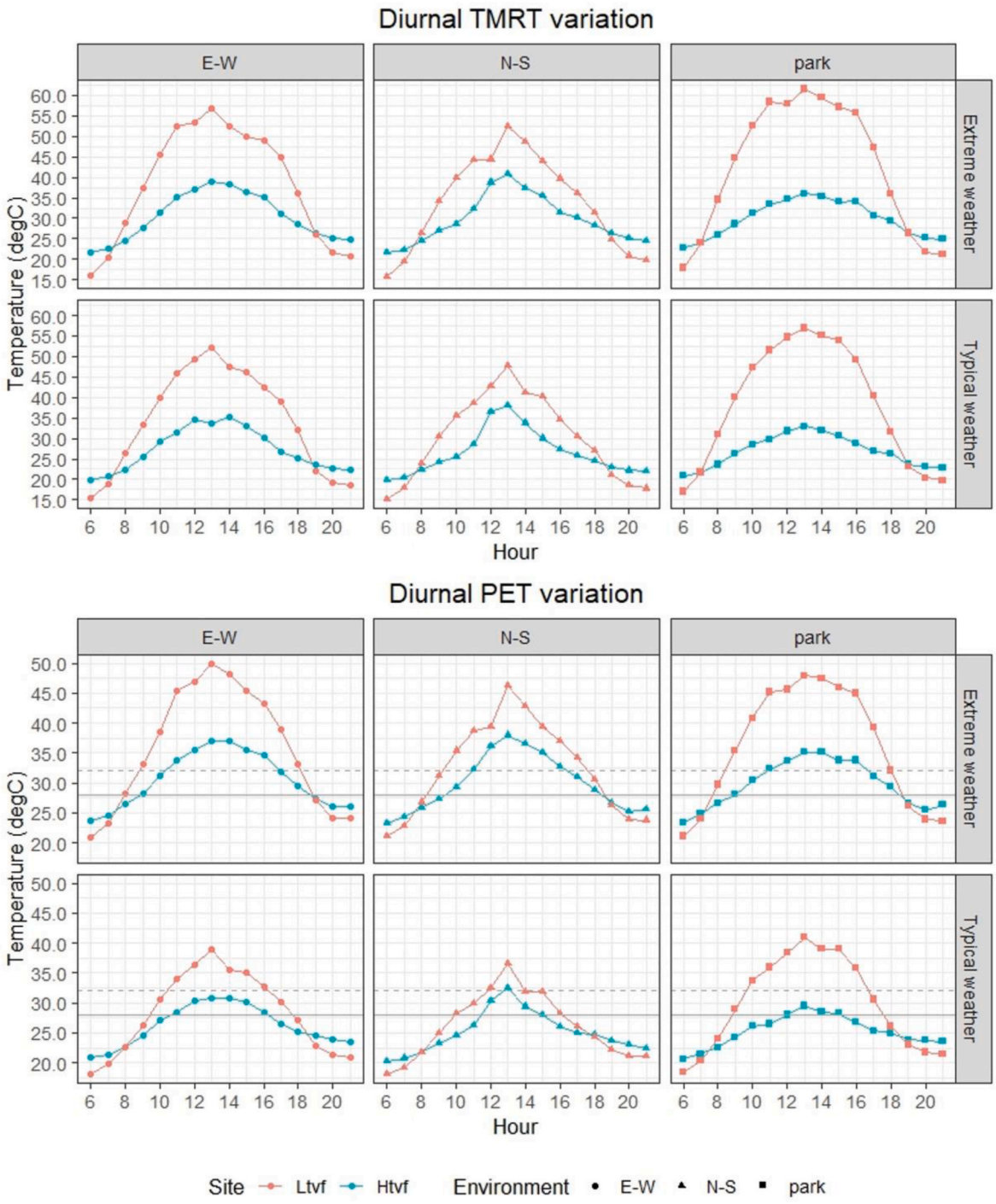

Fig. 8. Diurnal TMRT (top) and PET (bottom) variation in different urban environments under the two weather conditions. For PET, the solid horizontal line indicates the neutral PET of 28 °C, while the dotted horizontal line at 32 °C indicates the beginning of non-ideal thermal stress. DegC refers to the unit of temperature (°C).

3.2.4. PET

Fig. 8 (bottom) displays the diurnal variations of PET under different weather conditions. The similar pattern of PET to TMRT suggested that TMRT strongly influenced PET in Hong Kong summer. At Ltvf sites under typical weather, parks had the highest PET, followed by E-W and then N–S. At heatwave noon, E-W's Ltvf sites surprisingly had a higher PET than parks. Regarding Htvf sites, E-W generally had higher daytime PET than parks, while N–S had the lowest PET (except at noon). Another point to note was that under typical weather, pedestrians were suggested to stay under trees as the shade could provide a more thermally comfortable environment for outdoor activities. If it was not feasible, staying inside an N–S canyon could be an alternative. Although N–S had a non-ideal thermal condition around noon, PET inside N–S was within the ideal thermal stress threshold for most daytime under typical weather.

Fig. 8 (bottom) also shows the maximum PET reduction in the three urban environments. Under typical weather, parks had the highest values (11.4 °C), followed by E-W (8.1 °C) and then N–S (3.9 °C). However, this pattern changed during heatwaves. The diurnal PET reduction by trees at E-W (13.0 °C) was similar to the park one (12.8 °C),

while the value of N–S remained the lowest. The substantial increase in the maximum PET reduction was only observed in street canyons during heatwave events. It implied that the thermal sensation differences between Ltvf and Htvf sites might deteriorate in deep street canyons during a heatwave event.

3.3. Influence of tree and urban morphology on PET

3.3.1. Overall

Table 6 summarises the six multiple linear regression models analysed with 120 sites. The result showed that TVF was significant in all six models. BVFc was also significant except for the noon case under typical weather (12typ). Comparing the significance values (Pr(>|t)), TVF's was smaller than BVFc's in the same model. Besides, TVF had a more negative coefficient during noon and the afternoon, implying TVF had a larger PET reduction than BVFc when the daytime outdoor thermal comfort was the most uncomfortable.

Therefore, although BVFc (representing the urban morphology and geometry) was significantly causing an impact, the influence of TVF could be considered generally larger in the 120 sites, particularly during noon and the afternoon.

3.3.2. Special urban environments

Table 7 shows the summary of the six multiple linear regression models, analysed with a total of 30 sites in the E-W, N–S and parks. The results showed that TVF was significant in all six models. BVFc was insignificant in the noon and afternoon cases (insignificant in PET_12typ, PET_12ex, and PET_15ex). Comparing the cases in which both independent variables were significant, TVF had a smaller significance value (Pr(>|t)) than BVFc with a similar coefficient (except PET_09typ).

Therefore, it implied a more significant influence of TVF, particularly at noon and afternoon under extreme weather.

4. Discussion

4.1. Urban thermal comfort improvement by trees in different urban environments

There were two notable features shown among the three urban environments. First, parks had a larger TMRT reduction by trees than the other two urban environments. This was caused by the higher TMRT at Ltvf and low TMRT at Htvf sites at parks. Chen et al. [84] revealed that extremely high TMRT of a mean of 66.4 °C was experienced in unobstructed open areas in Shanghai. In Singapore, a metropolis with similar hot and humid climate as Hong Kong, Acero et al. [85] concluded that low-rise or partly open areas had a higher mean TMRT of 3.4 °C than the high-rise environments with the same street orientation in wet NE-Monsoon afternoons. Lau et al. [86] mentioned that open space generally received a higher TMRT than deep street canyons under the shading effect of surrounding buildings. In other words, urban parks generally had higher TMRT due to insufficient sheltering from insolation during the daytime. Lau et al. also highlighted that daytime TMRT inside deep street canyons could be 5 °C lower than inside the park [86]. Our study obtained a coherent outcome at Ltvf sites in parks and E-W. It further revealed that the TMRT differences between Ltvf sites in parks and N–S could reach 10 °C at noon and more in the rest of the daytime during heatwaves. Due to this fundamental difference in the TMRT at Ltvf sites, in addition to the lower TMRT observed at Htvf sites, parks had a larger TMRT reduction than the other two urban environments. Second, parks had a larger maximum PET reduction by trees (i.e. a larger reduction between Ltvf and Htvf sites in the park than in street canyons), resembling the above TMRT feature. The main reason was that TMRT had a decisive influence on the calculation of PET. As the absorbed shortwave and longwave radiation primarily affect human thermal comfort, the diurnal variations of PET in the outdoor environment were similar to the TMRT. Generally, the maximum PET reduction in parks was more prominent than in street canyons. Our results were consistent with Morakinyo et al. [38]. However, the interesting point was that the PET reduction in E-W was similar to the parks around noon during heatwaves.

Besides the PET magnitude, there was a longer thermal uncomfortable period (i.e., earlier to experience non-ideal thermal comfort in the morning and later to resume the ideal thermal comfort) at parks' Ltvf sites. Therefore, staying inside parks did not necessarily to be thermally comfortable. The sensible approach was to conduct outdoor activities at Htvf locations in parks to achieve ideal thermal comfort. Thus, the importance of designing shaded leisure areas is emphasised.

Street orientation was another critical factor controlling the TMRT and hence the thermal comfort within deep street canyons [50,87]. This research revealed two noteworthy features. First, E-W had more substantial TMRT reductions than N–S. In Ltvf sites, TMRT at E-W was higher than at N–S. In previous research conducted in locations having similar summer weather as Hong Kong (i.e., hot and humid summer weather), most concluded with echoing results [26,50,86,87]. While solar radiation could penetrate E-W during the daytime more easily, high-rise buildings along the N–S sheltered the pedestrian level from the insolation. Therefore, as trees planted inside the deep street canyon could reduce TMRT to a similar magnitude at Htvf sites regardless of road orientations, a larger cooling potential was found at E-W. Second, PET reduction in E-W was also larger than in N–S. At the pedestrian level, daytime PET in hot and humid summers was substantially influenced by solar radiation [39,88,89] and thus TMRT [39,90–92]. As daytime TMRT in E-W was higher at Ltvf sites, PET was generally higher, i.e., more deteriorated thermal comfort. In other words, there was a higher potential for PET reduction by trees in E-W.

In section 3, it was revealed that although trees reduced wind speeds at Htvf sites, which was consistent with previous research [93], the pedestrian-level thermal comfort improved. It was substantially contributed by the shading of tall trees, as demonstrated by the prominent TMRT reduction at Htvf sites. In other words, the advantages of planting trees to reach a high TVF in the urban area outweighed its disadvantages in a general high-density urban setting. Moreover, the improvement varied regarding different urban environments where the trees were planted.

In section 3.3, the multiple linear regression models suggested the significance of TVF in lowering the PET. Although urban morphology was reported as an important variable for changing urban climatic conditions, TVF also had a crucial influence on outdoor thermal comfort. The influence of TVF is especially essential at noon and afternoon. When solar radiation penetrates the deep street canyons due to the high

Table 6
Summary of the six multiple linear regression models analysed with 120 sites. Estimate refers to the coefficient. Pr(>|t) refers to the corresponding p-value.

Model	Variables	Estimate	Pr(>|t)	Model	Variables	Estimate	Pr(>|t)
PET_09typ	TVF	−2.8649	8.60e-10	**PET_09ex**	TVF	−5.7212	<2e-16
	BVFc	−4.8767	2.66e-04		BVFc	−6.7542	6.42e-09
PET_12typ	TVF	−9.4871	<2e-16	**PET_12ex**	TVF	−13.2127	<2e-16
	BVFc	−2.9109	0.178		BVFc	−4.4084	0.0311
PET_15typ	TVF	−8.8424	<2e-16	**PET_15ex**	TVF	−12.0864	<2e-16
	BVFc	−7.0873	4.12e-04		BVFc	−8.2967	0.0018

Table 7
Summary of the six multiple linear regression models, analysed with a total of 30 sites in the E-W, N–S and parks. Estimate refers to the coefficient. Pr(>|t) refers to the corresponding p-value.

Model	Variables	Estimate	Pr(>|t)	Model	Variables	Estimate	Pr(>|t)
PET_09typ	TVF	−4.0327	4.72e-05	**PET_09ex**	TVF	−7.376	1.53e-11
	BVFc	−7.3379	6.20e-04		BVFc	−7.7243	2.32e-05
PET_12typ	TVF	−9.449	1.67e-06	**PET_12ex**	TVF	−12.675	1.80e-09
	BVFc	−5.257	0.148		BVFc	−3.53	0.287
PET_15typ	TVF	−9.633	1.79e-07	**PET_15ex**	TVF	−12.354	5.27e-08
	BVFc	−10.245	0.00306		BVFc	−7.583	0.0546

elevation of the sun (in the summer), the direct overhead tree canopy at street level can shade pedestrians from shortwave solar radiation. This study emphasised the importance of overhead tree canopy shading as a small-scale mitigation and immediate shelter from solar radiation in a high-rise and high-density city.

4.2. GCR and TVF

Under the current greening policy in Hong Kong, a site's GCR should achieve 20% or 30% (for sites with areas of 1000–20,000 m^2 or greater than 20,000 m^2, respectively) [94] by applying a combination of greenery at different platforms (including roof, façade, podium, slopes, and water integration) with diverse vegetation species. Similarly, green factors in other regions, such as Seattle Green Factor and London Urban Greening Factors, were developed to assess the urban environment based on the total coverage area of various urban greenery types.

Although GCR is simple, straightforward, and easy to use, it ignores individual vegetation species' cooling effectiveness and efficiency. Rooftop greening had little influence on the air temperature and outdoor thermal comfort at the pedestrian level in high-rise metropolises with a hot and humid climate [95–98]. Vertical greening had a limited horizontal cooling scope [99,100] and Katsoulas et al. [100] reported that the inflection point was only 2.5 m. Therefore, not every green infrastructure included in GCR necessarily has pronounced improvement to the pedestrian-level thermal environment. Regarding ground-level vegetation, it was reported that the increase in grass coverage generally had a limited mitigation effect on thermal comfort at the pedestrian level [33,101,102]. Zhao et al. illustrated that the reduction in PET by grass only ranged from 3.8 to 4.7 °C with a GCR of 8%–56% compared to the base case of 0% GCR. However, for the scenario with a high-density canopy tree, the PET reduction ranged from 5.2 to 11.4 °C [33]. In similar biometeorological studies, the general conclusion was that a higher tree proportion in GCR could lead to a more thermally comfortable urban environment [33,37,38,101,103,104]. Research by Morakinyo et al. [37] proposed that TMRT reduction could be ranged from 5.6 °C to 9.1 °C, and the PET reduction could reach 3.2 °C–4.2 °C if there is 30% tree coverage regardless of tree species. Ma et al. [101] suggested that PET reduction of 0.78 °C could be achieved by increasing 3% the tree coverage ratio within the range of 3.5%–18.2% at 15:00. This implied that the prominent differences in thermal comfort at the pedestrian level could be due to the dominant vegetation types in the surrounding ground-level environment.

The dominant vegetation type is a decisive factor in human biometeorology due to the cooling mechanisms of vegetation. Urban greenery has three mechanisms to cool the thermal environment: shade provision, evapotranspiration, and increased albedo [7]. Although grass coverage at the street level can reduce the surface temperature by the latter two mechanisms, the limited height of grass restricts its effectiveness of shade provision. Thus, grass cannot effectively block solar radiation in urban environments at pedestrian heights. However, shade provision by trees improves the urban thermal environment. When pedestrians are under the tree shade, their shortwave radiation exposure reduces due to the reflection and absorption by the tree canopy. It helps to control the amount of absorbed solar radiation by the human body and affects the human energy budget. Reduced human heat stress load promotes thermal comfort, preventing the overheating of the body. As a result, tree shade provides the most prominent benefit of urban greenery to human biometeorology. Therefore, GCR, estimating the greenery coverage without considering the vegetation species, should not be the only morphological parameter analysed in urban microclimate and thermal sensation studies. Also, GCR target fulfilment should not be the only consideration when formulating the greenery policy in high-density metropolises.

Differing from GCR, TVF is a morphological parameter considering trees merely. In limited TVF research in regions with similar climates to Hong Kong, the general conclusion was that a higher TVF value (i.e., more overhead tree cover) led to a more substantial cooling effect and a thermally comfortable environment for pedestrians [40,50,105,106]. Zaki et al. [50] reported a reduction of 18.7 °C in TMRT and 10.6 °C in PET under a dense canopy, while a reduction of 15.7 °C in TMRT and 8.5 °C in PET were found under a sparse tree canopy when compared with the reference station. The results of this study were similar. Besides, the recent studies in other climates regions also coherently concluded on the relationship of TVF with various weather elements [45,46] or other outdoor thermal comfort indices [44,47]. It implies the importance of trees in regulating the outdoor thermal comfort of pedestrians in both microclimatic and psychological [41] contexts across different climates.

As observed from the results of previous literature and Figure S3, a high TVF did not necessarily represent a high GCR value. TVF of a site depends on its immediate surrounding above the pedestrian, whereas GCR depends on the ground-level environment within a selected buffer size. Therefore, when pedestrians travel across a region, TVF may substantially vary while GCR remains similar, especially when individual roadside trees are common in a compact city. On the other hand, TMRT and PET depend on exposure to solar radiation, which is also greatly influenced by the immediate shading provided by urban structures. In other words, TMRT and PET can also vary substantially in a short distance. Table S1 summarises the correlations between PET and TVF/GCR. It showed that PET and TVF generally had a significant negative correlation in different districts under both typical and extreme weather. Meanwhile, generally insignificant correlations were found between PET and GCR in the six locations independently (Tables S2–S7). Generally insignificant correlations were also found between TA and TVF or GCR. Hence, using TVF as the morphology parameter may capture the variations better than GCR when studying weather parameters that greatly vary in spatial distribution, such as TMRT and PET. Moreover, as concluded in previous research, tree shade was directly related to human sensation and the perception towards thermal comfort, affecting the behavioural adaptation of pedestrians. Cheung and Jim [107] concluded that the average useable time of a tree-shaded site approximately doubled when compared to a well-exposed site in Kowloon Bay, Hong Kong. Another study by Lo et al. [108] in Hong Kong proposed that 95% of survey respondents recognised urban tree shade provision, and 93.6% affirmed the contribution of the cooling effect of trees. Chan et al. [109] proposed that a higher level of thermal acceptability was found at the survey locations where trees were observable in situ. In research conducted at a square in Taichung City, a hot and humid city in central Taiwan, the most preferred mitigation of over 70% of respondents was to seek shading under trees [110]. Because of the above two main reasons, TVF may be a better indicator to quantify the relation

between trees and human thermal comfort.

4.3. Implications on urban design, and limitations

This study proposed and evaluated the use of TVF to quantify pedestrian thermal comfort in complex urban settings. It provides insights into the relevance of using the hemispheric view of tree cover at the pedestrian level to human thermal comfort. Our results showed that using TVF can better capture the shading effect in terms of the reduction in TMRT and PET as the main determinant of shading efficiency. This echoes the findings of our previous studies that foliage density accounts for 60% of temperature regulation [37]. Generally speaking, tree species with high foliage density are more preferred in reducing the heat load, but they are limited by the scarce land resources and the underground utilities commonly found in the urban environment. Selecting the right trees at appropriate locations was previously investigated [64]. TVF can therefore provide an indicator for choosing the appropriate and cooling-effective tree species according to the conditions of site contexts.

The findings of the present study can inform the current practices of tree planting or vegetation provision in Hong Kong. Chapter 4 of the Hong Kong Planning Standard and Guidelines concerning greening in the city focuses primarily on the areas of tree planting and the overall percentage of tree coverage in site development [111]. It provides general guidance for greenery provision in site planning. The Sustainable Building Design Guidelines also address the site coverage of greenery and take a step further on how the specific types of greenery account for the overall site coverage [94]. However, it does not provide specific guidance and evaluation at pedestrian-level landscape design. Considering the TVF in developing landscape design facilitates a paradigm shift from generalizing tree or greenery coverage to individual-based thermal comfort. It contributes to the revision of existing guidelines to include the concept of individual-based thermal comfort in tree design. It also offers flexibility to landscape and urban designers in selecting the appropriate and effective tree species according to the context of street environments.

This study had two limitations. First, the walls of buildings in the model domains were constructed solely with concrete for simplification. With this discrepancy, the street-level radiation budget in the model might differ from that in the actual urban environments [112,113]. To improve its accuracy, the building models in the simulation domain could be constructed with additional materials, such as glass, to avoid the over-simplification of actual buildings. Second, only two tree models were used in the domain for simplification. In the real-world environment, trees have different morphologies based on their species [40,114], so replacing them with other species might generate slightly different values [37]. Such replacement can evaluate the actual cooling effect of particular tree species on outdoor human comfort at the pedestrian level.

5. Conclusion

This research demonstrated the usage of TVF to investigate the relationship between trees and pedestrian thermal comfort. Through performing ENVI-met simulations in the six different high-rise and high-density locations in Hong Kong (a metropolis with hot and humid subtropical summer), air temperature, wind speed, TMRT, as well as PET (indicating the thermal comfort at the pedestrian level) were thoroughly studied under both typical and extreme weather (a heatwave event).

Results showed that although Htvf sites received similar air temperatures and reduced wind speeds compared to Ltvf sites, TMRT prominently reduced. Hence, the PET in Htvf sites remained below 32 °C (the ideal thermal comfort) under typical summer weather. This study also revealed that the above features remained similar under extreme weather, indicating that Htvf sites could help mitigate the substantial changes in temperatures and thermal comfort. Diurnal variations were also found within urban environments such as parks, E-W, and N–S street canyons. Although Ltvf sites in parks received more solar radiation than in deep street canyons, the cooling potential exhibited by parks' Htvf sites was more substantial than in street canyons. Moreover, Htvf sites experienced an improvement in thermal comfort when compared to Ltvf sites within the same deep street canyon. To conclude, Htvf sites at different locations and urban environments could maintain better thermal comfort for pedestrians due to the reduction in TMRT.

Therefore, this research demonstrated that tree shading was crucial to thermal comfort inside a high-rise and high-density metropolis with compact and mixed land uses. Keeping a high TVF in such a city could improve thermal comfort and help to lengthen the period ideal for outdoor activities under both typical and extreme weather, which could be more frequent in the future.

This study suggests that TVF is a suitable vegetation morphological parameter in complex urban settings and should also be considered and adopted as a crucial indicator for future urban development. Future urban landscape designs can consider keeping a continuous overhead tree canopy to maintain high TVF in the neighbourhood, thereby creating a thermally comfortable outdoor environment for pedestrians, especially for the elderly who are more vulnerable to extreme weather. Planting trees not only increase the TVF nearby but also fulfils the GCR target of mitigating the impact caused by future climate change. With additional applications of ventilation corridors, the effectiveness of this mitigation for future pedestrian thermal comfort could be further improved. The results of this research emphasise the importance of sheltering from solar radiation under a tree in order to achieve pedestrian thermal comfort when conducting outdoor activities.

CRediT authorship contribution statement

Ka Yuen Cheng: Writing – review & editingWriting – review & editing, Writing – original draftWriting – original draft, Visualization, Methodology, Investigation, Conceptualization. **Kevin Lau:** Writing – review & editingWriting – review & editing, Writing – original draftWriting – original draft, Conceptualization. **Ying Ting Shek:** Resources, Methodology. **Zhixin Liu:** Writing – review & editingWriting – review & editing, Methodology. **Edward Ng:** Writing – review & editingWriting – review & editing, Supervision, Project administration, Funding acquisition, Conceptualization.

Declaration of competing interest

The authors declare that they have no known competing financial interests or personal relationships that could have appeared to influence the work reported in this paper.

Data availability

Data will be made available on request.

Acknowledgements

This study is supported by the Research Impact Fund (Project Code: CUHK R4046-18) of the Research Grants Council, Hong Kong.

Appendix A. Supplementary data

Supplementary data to this article can be found online at https://doi.org/10.1016/j.buildenv.2023.110431.

References

[1] F.J. Doblas-Reyes, A.A. Sörensson, M. Almazroui, A. Dosio, W.J. Gutowski, R. Haarsma, R. Hamdi, B. Hewitson, W.-T. Kwon, B.L. Lamptey, D. Maraun, T. S. Stephenson, I. Takayabu, L. Terray, A. Turner, Z. Zuo, Linking global to regional climate change., in climate change 2021: the physical science basis, in: V. Masson-Delmotte, P. Zhai, A. Pirani, S.L. Connors, C. Péan, S. Berger, N. Caud,

Y. Chen, L. Goldfarb, M.I. Gomis, M. Huang, K. Leitzell, E. Lonnoy, J.B. R. Matthews, T.K. Maycock, T. Waterfield, O. Yelekçi, R. Yu, B. Zhou (Eds.), Contribution of Working Group I to the Sixth Assessment Report of the Intergovernmental Panel on Climate Change, 2021, pp. 1363–1512.
[2] Hong Kong Observatory, H.K.S.A.R, Ranking of temperature and rainfall recorded at the Hong Kong Observatory (Annual) [cited 2022 14 September]; Available from, https://www.hko.gov.hk/en/cis/statistic/erank.htm?month=13, 2021.
[3] Met Office, U.K. Unprecedented Extreme Heatwave, July 2022, p. 2022 [cited 2022 14 September]; Available from: https://www.metoffice.gov.uk/binaries/content/assets/metofficegovuk/pdf/weather/learn-about/uk-past-events/interesting/2022/2022_03_july_heatwave.pdf.
[4] S. Gu, et al., Heat-related illness in China, summer of 2013, Int. J. Biometeorol. 60 (1) (2016) 131–137.
[5] S. Jena, A. Gairola, Numerical method to generate and evaluate environmental wind over hills: comparison of pedestrian winds over hills and plains, CFD Lett. 14 (10) (2022) 56–67.
[6] E. Jamei, et al., Review on the impact of urban geometry and pedestrian level greening on outdoor thermal comfort, Renew. Sustain. Energy Rev. 54 (2016) 1002–1017.
[7] N.H. Wong, et al., Greenery as a mitigation and adaptation strategy to urban heat, Nat. Rev. Earth Environ. 2 (3) (2021) 166–181.
[8] K.K.-L. Lau, S.C. Chung, C. Ren, Outdoor thermal comfort in different urban settings of sub-tropical high-density cities: an approach of adopting local climate zone (LCZ) classification, Build. Environ. 154 (2019) 227–238.
[9] M. Cetin, et al., Evaluation of thermal climatic region areas in terms of building density in urban management and planning for Burdur, Turkey, Air Qual. Atmos. Health 12 (9) (2019) 1103–1112.
[10] Block, A.H., S.J. Livesley, and N.S.G. Williams, Responding to the urban heat island: a review of the potential of green infrastructure. 2012, the Victorian Centre for Climate Change Adaptation..
[11] F. Balany, et al., Green infrastructure as an urban heat island mitigation strategy—a review, Water 12 (12) (2020) 3577.
[12] S. Zheng, et al., Influence of trees on the outdoor thermal environment in subtropical areas: an experimental study in Guangzhou, China, Sustain. Cities Soc. 42 (2018) 482–497.
[13] C.Y. Jim, Thermal performance of climber greenwalls: effects of solar irradiance and orientation, Appl. Energy 154 (2015) 631–643.
[14] L.L. Peng, C.Y. Jim, Green-roof effects on neighborhood microclimate and human thermal sensation, Energies 6 (2) (2013) 598–618.
[15] Y. Wang, U. Berardi, H. Akbari, Comparing the effects of urban heat island mitigation strategies for Toronto, Canada, Energy Build. 114 (2016) 2–19.
[16] G. Battista, R. de Lieto Vollaro, M. Zinzi, Assessment of urban overheating mitigation strategies in a square in Rome, Italy, Sol. Energy 180 (2019) 608–621.
[17] T. Zölch, et al., Using green infrastructure for urban climate-proofing: an evaluation of heat mitigation measures at the micro-scale, Urban For. Urban Green. 20 (2016) 305–316.
[18] A.L. Pisello, et al., Facing the urban overheating: recent developments. Mitigation potential and sensitivity of the main technologies, Wiley Interdiscip. Rev. Energy Environ. 7 (4) (2018) p. n/a.
[19] H. Saaroni, et al., Urban Green Infrastructure as a tool for urban heat mitigation: survey of research methodologies and findings across different climatic regions, Urban Clim. 24 (2018) 94–110.
[20] C. Wang, Z.H. Wang, J. Yang, Cooling effect of urban trees on the built environment of contiguous United States, Earth's Future 6 (8) (2018) 1066–1081.
[21] N. Meili, et al., Tree effects on urban microclimate: diurnal, seasonal, and climatic temperature differences explained by separating radiation, evapotranspiration, and roughness effects, Urban For. Urban Green. 58 (2021), 126970.
[22] G.Y. Qiu, et al., Experimental studies on the effects of green space and evapotranspiration on urban heat island in a subtropical megacity in China, Habitat Int. 68 (2017) 30–42.
[23] L. Kong, et al., Regulation of outdoor thermal comfort by trees in Hong Kong, Sustain. Cities Soc. 31 (2017) 12–25.
[24] W. Yang, Y. Lin, C.-Q. Li, Effects of landscape design on urban microclimate and thermal comfort in tropical climate, Adv. Meteorol. (2018) 1–13, 2018.
[25] S.A. Zaki, et al., Effects of urban morphology on microclimate parameters in an urban university campus, Sustain. Basel 12 (7) (2020) 2962.
[26] S. Yin, et al., Correlative impact of shading strategies and configurations design on pedestrian-level thermal comfort in traditional shophouse neighbourhoods, Southern China, Sustain. Basel 11 (5) (2019) 1355.
[27] T. Chen, et al., Effects of tree plantings and aspect ratios on pedestrian visual and thermal comfort using scaled outdoor experiments, Sci. Total Environ. 801 (2021) 149527, 149527.
[28] P.K. Cheung, C.K.W. Fung, C.Y. Jim, Seasonal and meteorological effects on the cooling magnitude of trees in subtropical climate, Build. Environ. 177 (2020) 106911.
[29] A. Ghaffarianhoseini, et al., Analyzing the thermal comfort conditions of outdoor spaces in a university campus in Kuala Lumpur, Malaysia, Sci. Total Environ. 666 (2019) 1327–1345.
[30] R. Andhy Bato, H. Hayati Sari, S. Ahyahudin, Thermal comfort-based spatial planning Model in Jakarta Transit-oriented development (TOD), Atmosphere 13 (565) (2022) 565.
[31] P. Mohammad, et al., Evaluating the role of the albedo of material and vegetation scenarios along the urban street canyon for improving pedestrian thermal comfort outdoors, Urban Clim. 40 (2021), 100993.
[32] P.K. Cheung, C.Y. Jim, Differential cooling effects of landscape parameters in humid-subtropical urban parks, Landsc. Urban Plann. 192 (2019), 103651.
[33] T.F. Zhao, K.F. Fong, Characterization of different heat mitigation strategies in landscape to fight against heat island and improve thermal comfort in hot-humid climate (Part II): evaluation and characterization, Sustain. Cities Soc. 35 (2017) 841–850.
[34] H. Li, et al., Analysis of cooling and humidification effects of different coverage types in small green spaces (SGS) in the context of urban homogenization: a case of HAU campus green spaces in summer in Zhengzhou, China, Atmosphere-Basel 11 (8) (2020) 862.
[35] J. Zhang, Z. Gou, L. Shutter, Effects of internal and external planning factors on park cooling intensity: field measurement of urban parks in Gold Coast, Australia, AIMS Environ. Sci. 6 (6) (2019) 417–434.
[36] Z. Liu, et al., The effect of trees on human energy fluxes in a humid subtropical climate region, Int. J. Biometeorol. 64 (10) (2020) 1675–1686.
[37] T.E. Morakinyo, et al., Performance of Hong Kong's common trees species for outdoor temperature regulation, thermal comfort and energy saving, Build. Environ. 137 (2018) 157–170.
[38] T.E. Morakinyo, et al., A study on the impact of shadow-cast and tree species on in-canyon and neighborhood's thermal comfort, Build. Environ. 115 (2017) 1–17.
[39] J. Wu, H. Chang, S. Yoon, Numerical study on microclimate and outdoor thermal comfort of street canyon Typology in extremely hot weather—a case study of busan, South Korea, Atmosphere-Basel 13 (2) (2022) 307.
[40] L.V. de Abreu-Harbich, L.C. Labaki, A. Matzarakis, Effect of tree planting design and tree species on human thermal comfort in the tropics, Landsc. Urban Plan 138 (2015) 99–109.
[41] L. Xiang, et al., Modeling pedestrian emotion in high-density cities using visual exposure and machine learning: Tracking real-time physiology and psychology in Hong Kong, Build. Environ. 205 (2021), 108273.
[42] F. Xue, S.S.Y. Lau, Climate-adaptive urban open space design strategy in workplace for comfort and health-case in Hong Kong and Singapore, Procedia Eng. 169 (2016) 332–339.
[43] G. Li, et al., Evaluation strategies on the thermal environmental effectiveness of street canyon clusters: a case study of harbin, China, Sustainability 14 (13013) (2022) 13013.
[44] M.A. Ruiz, et al., Design tool to improve daytime thermal comfort and nighttime cooling of urban canyons, Landsc. Urban Plann. 167 (2017) 249–256.
[45] E.-S. Kim, et al., Estimation of mean radiant temperature in urban canyons using google street view: a case study on Seoul, Rem. Sens. 14 (2) (2022) 260.
[46] N.D. Yıldız, et al., Analyzing the effect of view factors on surface heat flux, surface temperature, and vegetation cover, Environ. Sci. Pollut. Control Ser. 30 (15) (2023) 43843–43859.
[47] O. Hisato, et al., Risk assessment of heat stroke during the marathon of the Tokyo 2020 Olympics in Sapporo, Hokkaido, Sustainability 15 (5) (2023) 3997.
[48] K. Wang, et al., Assessing effects of urban greenery on the regulation mechanism of microclimate and outdoor thermal comfort during winter in China's cold region, Land 11 (1442) (2022) 1442.
[49] X. Deng, et al., Influence of built environment on outdoor thermal comfort: a comparative study of new and old urban blocks in Guangzhou, Build. Environ. (2023), 110133.
[50] S.A. Zaki, et al., Effects of roadside trees and road orientation on thermal environment in a tropical City, Sustain. Basel 12 (3) (2020) 1053.
[51] Census and Statistics Department, H.K.S.A.R., Hong Kong in Figures, 2022. page 5.
[52] E. Ng, et al., Improving the wind environment in high-density cities by understanding urban morphology and surface roughness: a study in Hong Kong, Landsc. Urban Plann. 101 (1) (2011) 59–74.
[53] M.C. Peel, B.L. Finlayson, T.A. McMahon, Updated world map of the Köppen-Geiger climate classification, Hydrol. Earth Syst. Sci. 11 (5) (2007) 1633–1644.
[54] Hong Kong Observatory, H.K.S.A.R, Monthly meteorological normals for Hong Kong (1991-2020), Available from, https://www.hko.gov.hk/en/cis/normal/1991_2020/normals.htm, 2021.
[55] Hong Kong Observatory, H.K.S.A.R, Climate of Hong Kong, Available from, https://www.hko.gov.hk/en/cis/climahk.htm, 2022.
[56] Hong Kong Observatory, H.K.S.A.R, What is "heatwave"? Educational resources, Available from, https://www.hko.gov.hk/en/education/weather/hot-and-cold-weather/00661-What-is-Heatwave.html, 2021.
[57] Hong Kong Observatory, H.K.S.A.R, Warnings and signals database: very hot weather warning. 2020 [cited 2022 14 September]; Available from, https://www.hko.gov.hk/en/wxinfo/climat/warndb/warndb13.shtml?opt=13&start_ym=201709&end_ym=202209&submit=%E6%90%9C%E5%B0%8B, 9 January 2020.
[58] Hong Kong Observatory, H.K.S.A.R, Daily maximum temperature (°C) at the Hong Kong observatory 2020. Daily data for single element 2021 [cited 2022 14 September]; Available from, https://www.hko.gov.hk/en/cis/dailyElement.htm?ele=MAX_TEMP&y=2020, 29 July 2021.
[59] H. Lan, et al., Improved urban heat island mitigation using bioclimatic redevelopment along an urban waterfront at Victoria Dockside, Hong Kong, Sustain. Cities Soc. 74 (2021), 103172.
[60] M. Bruse, ENVI-met 3.0: Updated Model Overview. https://www.researchgate.net/publication/238622880_ENVI-met_30_Updated_Model_Overview.
[61] S. Tsoka, et al., Urban warming and cities' microclimates: Investigation methods and mitigation strategies—a review, Energies 13 (6) (2020) 1414.
[62] T.E. Morakinyo, et al., Thermal benefits of vertical greening in a high-density city: case study of Hong Kong, Urban For. Urban Green. 37 (2019) 42–55.
[63] Z. Tan, K.K.-L. Lau, E. Ng, Urban tree design approaches for mitigating daytime urban heat island effects in a high-density urban environment, Energy Build. 114 (2016) 265–274.

[64] T.E. Morakinyo, et al., Right tree, right place (urban canyon): tree species selection approach for optimum urban heat mitigation - development and evaluation, Sci. Total Environ. 719 (2020), 137461.
[65] Z. Tan, K.K.-L. Lau, E. Ng, Planning strategies for roadside tree planting and outdoor comfort enhancement in subtropical high-density urban areas, Build. Environ. 120 (2017) 93–109.
[66] W. Ouyang, et al., Evaluating the thermal-radiative performance of ENVI-met model for green infrastructure typologies: experience from a subtropical climate, Build. Environ. 207 (2022), 108427.
[67] Z.I. Janjic, A nonhydrostatic model based on a new approach, Meteorol. Atmos. Phys. 82 (1–4) (2003) 271–285.
[68] Y.T. Kwok, et al., High-resolution mesoscale simulation of the microclimatic effects of urban development in the past, present, and future Hong Kong, Urban Clim. 37 (2021), 100850.
[69] Y. Xu, et al., Urban morphology detection and computation for urban climate research, Landsc. Urban Plann. 167 (2017) 212–224.
[70] Y. Shi, et al., Identifying critical building morphological design factors of street-level air pollution dispersion in high-density built environment using mobile monitoring, Build. Environ. 128 (2018) 248–259.
[71] Y. Shi, K.K.-L. Lau, E. Ng, Developing street-level PM2.5 and PM10 land use regression models in high-density Hong Kong with urban morphological factors, Environ. Sci. Technol. 50 (15) (2016) 8178–8187.
[72] T.R. Oke, G. Mills, A. Christen, J.A. Voogt, in: Urban ClimatesA. Christen, et al. (Eds.), Concepts, Cambridge University Press, Cambridge, 2017, pp. 14–43.
[73] P.P.-Y. Wong, et al., The impact of environmental and human factors on urban heat and microclimate variability, Build. Environ. 95 (2016) 199–208.
[74] R. Beelen, et al., Development of NO2 and NOx land use regression models for estimating air pollution exposure in 36 study areas in Europe – the ESCAPE project, Atmos. Environ. 2013 (72) (1994) 10–23.
[75] P. Hoppe, The physiological equivalent temperature - a universal index for the biometeorological assessment of the thermal environment, Int. J. Biometeorol. 43 (2) (1999) 71–75.
[76] E. Walther, Q. Goestchel, The P.E.T. comfort index: questioning the model, Build. Environ. 137 (2018) 1–10.
[77] Z. Liu, et al., Heat mitigation benefits of urban green and blue infrastructures: a systematic review of modeling techniques, validation and scenario simulation in ENVI-met, Build. Environ. 200 (2021), 107939, V4.
[78] Y. Wu, K. Graw, A. Matzarakis, Comparison of thermal comfort between sapporo and Tokyo—the case of the Olympics 2020, Atmosphere 11 (5) (2020) 444.
[79] S. Thorsson, et al., Potential changes in outdoor thermal comfort conditions in Gothenburg, Sweden due to climate change: the influence of urban geometry, Int. J. Climatol. 31 (2) (2011) 324–335.
[80] E. Ng, V. Cheng, Urban human thermal comfort in hot and humid Hong Kong, Energy Build. 55 (2012) 51–65.
[81] V. Cheng, et al., Outdoor thermal comfort study in a sub-tropical climate: a longitudinal study based in Hong Kong, Int. J. Biometeorol. 56 (1) (2011) 43–56.
[82] L. Chen, et al., Sky view factor analysis of street canyons and its implications for daytime intra-urban air temperature differentials in high-rise, high-density urban areas of Hong Kong: a GIS-based simulation approach, Int. J. Climatol. 32 (1) (2012) 121–136.
[83] Z. Liu, et al., Microclimatic measurements in tropical cities: systematic review and proposed guidelines, Build. Environ. 222 (2022), 109411.
[84] L. Chen, et al., Intra-urban differences of mean radiant temperature in different urban settings in Shanghai and implications for heat stress under heat waves: a GIS-based approach, Energy Build. 130 (2016) 829–842.
[85] J.A. Acero, et al., Quantifying the effect of building shadowing and cloudiness on mean radiant temperature in Singapore, Atmosphere 12 (8) (2021) 1012.
[86] K.K.-L. Lau, et al., Numerical modelling of mean radiant temperature in high-density sub-tropical urban environment, Energy Build. 114 (2016) 80–86.
[87] F.-Y. Gong, et al., Spatiotemporal patterns of street-level solar radiation estimated using Google Street View in a high-density urban environment, Build. Environ. 148 (2019) 547–566.
[88] T.E. Morakinyo, Y.F. Lam, Simulation study on the impact of tree-configuration, planting pattern and wind condition on street-canyon's micro-climate and thermal comfort, Build. Environ. 103 (2016) 262–275.
[89] K. Li, X. Li, K. Yao, Outdoor thermal environments of main types of urban areas during summer: a field study in Wuhan, China, Sustain. Basel 14 (2) (2022) 952.
[90] D. Hartabela, B.J. Dewancker, M.D. Koerniawan, A relationship between micro-meteorological and personal variables of outdoor thermal comfort: a case study in kitakyushu, Japan, Sustain. Basel 13 (24) (2021) 13634.
[91] Z. Tan, et al., Design for climate resilience: influence of environmental conditions on thermal sensation in subtropical high-density cities, Architect. Sci. Rev. 62 (1) (2019) 3–13.
[92] N.E. Othman, et al., Field study of pedestrians' comfort temperatures under outdoor and semi-outdoor conditions in Malaysian university campuses, Int. J. Biometeorol. 65 (4) (2021) 453–477.
[93] F. Yang, F. Qian, S.S.Y. Lau, Urban form and density as indicators for summertime outdoor ventilation potential: a case study on high-rise housing in Shanghai, Build. Environ. 70 (2013) 122–137.
[94] Buildings Department, H.K.S.A.R, Sustain. Build. Des. Guidel. (2016). HKSAR.
[95] E. Ng, et al., A study on the cooling effects of greening in a high-density city: an experience from Hong Kong, Build. Environ. 47 (1) (2012) 256–271.
[96] L.L.H. Peng, C.Y. Jim, Green-roof effects on neighborhood microclimate and human thermal sensation, Energies 6 (2) (2013) 598–618.
[97] T.E. Morakinyo, et al., Temperature and cooling demand reduction by green-roof types in different climates and urban densities: a co-simulation parametric study, Energy Build. 145 (2017) 226–237.
[98] S. Guo, F. Yang, Z. Jiang, Thermal environmental effects of vertical greening and building layout in open residential neighbourhood design: a case study in Shanghai, Architect. Sci. Rev. 65 (1) (2022) 72–88.
[99] T.E. Morakinyo, et al., Thermal benefits of vertical greening in a high-density city: case study of Hong Kong, Urban For. Urban Green. 37 (2019) 42–55.
[100] N. Katsoulas, et al., Microclimatic effects of planted hydroponic structures in urban environment: measurements and simulations, Int. J. Biometeorol. 61 (5) (2017) 943–956.
[101] X. Ma, et al., Performance of different urban design parameters in improving outdoor thermal comfort and health in a pedestrianized zone, Int. J. Environ. Res. Publ. Health 17 (7) (2020) 2258.
[102] X. Ma, et al., The effect of various urban design parameter in alleviating urban heat island and improving thermal health—a case study in a built pedestrianized block of China, Environ. Sci. Pollut. Res. 28 (28) (2021) 38406–38425.
[103] W. Ouyang, et al., The cooling efficiency of variable greenery coverage ratios in different urban densities: a study in a subtropical climate, Build. Environ. 174 (2020), 106772.
[104] J.-M. Huang, L.-C. Chen, A numerical study on mitigation strategies of urban heat islands in a tropical megacity: a case study in Kaohsiung city, Taiwan, Sustain. Basel 12 (10) (2020) 3952.
[105] Y.J. Kim, R.D. Brown, A multilevel approach for assessing the effects of microclimatic urban design on pedestrian thermal comfort: the High Line in New York, Build. Environ. 205 (2021) 108244.
[106] J. Wei, et al., The cooling and humidifying effects and the thresholds of plant community structure parameters in urban aggregated green infrastructure, Forests 12 (2) (2021) 1–16.
[107] P.K. Cheung, C.Y. Jim, Subjective outdoor thermal comfort and urban green space usage in humid-subtropical Hong Kong, Energy Build. 173 (2018) 150–162.
[108] A.Y. Lo, J.A. Byrne, C.Y. Jim, How climate change perception is reshaping attitudes towards the functional benefits of urban trees and green space: lessons from Hong Kong, Urban For. Urban Green. 23 (2017) 74–83.
[109] S.Y. Chan, C.K. Chau, T.M. Leung, On the study of thermal comfort and perceptions of environmental features in urban parks: a structural equation modeling approach, Build. Environ. 122 (2017) 171–183.
[110] T.-P. Lin, Thermal perception, adaptation and attendance in a public square in hot and humid regions, Build. Environ. 44 (10) (2009) 2017–2026.
[111] Planning Department, H.K.S.A.R., in: H.K.S.A.R. Planning Department (Ed.), Chapter 4 Recreation, Open Space & Greening, 2015. HKSAR.
[112] N. Nazarian, et al., Effectiveness of cool walls on cooling load and urban temperature in a tropical climate, Energy Build. 187 (2019) 144–162.
[113] J. Li, et al., Cooling and energy-saving performance of different green wall design: a simulation study of a block, Energies 12 (15) (2019) 2912.
[114] Y.-H. Lin, K.-T. Tsai, Screening of tree species for improving outdoor human thermal comfort in a Taiwanese City, Sustain. Basel 9 (3) (2017) 340.